Vps Factors Are Required for Efficient Transcription Elongation in Budding Yeast

Naseem A. Gaur,*[,1] Jiri Hasek,[†] Donna Garvey Brickner,[‡] Hongfang Qiu,* Fan Zhang,* Chi-Ming Wong,*[,2] Ivana Malcova,[†] Pavla Vasicova,[†] Jason H. Brickner,[‡] and Alan G. Hinnebusch*[,3]

*Laboratory of Gene Regulation and Development, Eunice K. Shriver National Institute of Child Health and Human Development, National Institutes of Health, Bethesda, Maryland 20892, [†]Laboratory of Cell Reproduction, Institute of Microbiology, Academy of Sciences of the Czech Republic, 142 20 Prague, Czech Republic, and [‡]Department of Molecular Biosciences, Northwestern University, Evanston, Illinois 60208

ABSTRACT There is increasing evidence that certain Vacuolar protein sorting (Vps) proteins, factors that mediate vesicular protein trafficking, have additional roles in regulating transcription factors at the endosome. We found that yeast mutants lacking the phosphatidylinositol 3-phosphate [PI(3)P] kinase Vps34 or its associated protein kinase Vps15 display multiple phenotypes indicating impaired transcription elongation. These phenotypes include reduced mRNA production from long or G+C-rich coding sequences (CDS) without affecting the associated *GAL1* promoter activity, and a reduced rate of RNA polymerase II (Pol II) progression through *lacZ* CDS *in vivo*. Consistent with reported genetic interactions with mutations affecting the histone acetyltransferase complex NuA4, *vps15Δ* and *vps34Δ* mutations reduce NuA4 occupancy in certain transcribed CDS. *vps15Δ* and *vps34Δ* mutants also exhibit impaired localization of the induced *GAL1* gene to the nuclear periphery. We found unexpectedly that, similar to known transcription elongation factors, these and several other Vps factors can be cross-linked to the CDS of genes induced by Gcn4 or Gal4 in a manner dependent on transcriptional induction and stimulated by Cdk7/Kin28-dependent phosphorylation of the Pol II C-terminal domain (CTD). We also observed colocalization of a fraction of Vps15-GFP and Vps34-GFP with nuclear pores at nucleus–vacuole (NV) junctions in live cells. These findings suggest that Vps factors enhance the efficiency of transcription elongation in a manner involving their physical proximity to nuclear pores and transcribed chromatin.

NEWLY synthesized proteins that are transported from the Golgi to the lysosome/vacuole traverse the endosome, as do ubiquitinated proteins that are removed from the plasma membrane by endocytosis *en route* to the vacuole for degradation. Ubiquitinated cargo proteins progress through early and late endosomes, are concentrated at the outer membranes of multivesicular bodies (MVB), and are then sequestered in intralumenal vesicles (ILVs) of the MVB. Fusion of the MVB with the vacuole delivers cargo proteins to the vacuole lumen for degradation by vacuolar hydrolases. "Class C and D" Vacuolar protein sorting (Vps) factors participate in vesicle fusion at the endosome, while cargo sorting and delivery to the ILVs at the MVB involves class E Vps proteins, including the components of the soluble ESCRT (endosomal sorting complex required for transport) complexes ESCRT-0, -I, -II, and -III (Bowers and Stevens 2005; Hurley and Emr 2006; Raiborg and Stenmark 2009).

It is thought that ESCRT-0 is recruited from the cytoplasm to the endosomal outer membrane by interaction with the phosphoinositide PI(3)P, where it acts to recruit and concentrate ubiquitinated cargo proteins and transfer them to the ESCRT-I complex. ESCRT-I activates the ESCRT-II heterotrimer that, in turn, recruits the ESCRT-III components, which are believed to assemble filaments instrumental in invagination of the MVB membrane. The AAA-ATPase Vps4, recruited by ESCRT-III subunits, functions to pinch off the membrane invaginations to produce ILVs containing cargo proteins and to recycle the ESCRT factors back to the cytoplasm (Raiborg and Stenmark 2009).

doi: 10.1534/genetics.112.146308
Manuscript received September 28, 2012; accepted for publication January 9, 2013
Supporting information is available online at http://www.genetics.org/lookup/suppl/doi:10.1534/genetics.112.146308/-/DC1.
[1]Present address: Synthetic Biology and Biofuel Group, International Centre for Genetic Engineering and Biotechnology (ICGEB), Aruna Asaf Ali Marg, New Delhi 110067.
[2]Present address: Department of Medicine, University of Hong Kong, Hong Kong.
[3]Corresponding author: Eunice K. Shriver National Institute of Child Health and Human Development, NIH, Bldg. 6A, Room B1A13, Bethesda, MD 20874. E-mail: ahinnebusch@nih.gov

There is increasing evidence that certain Vps proteins have additional functions in cytoplasmic signaling pathways that regulate transcription in the nucleus. In budding yeast, ESCRT-III factor Snf7/Vps32 and the subunits of ESCRT-II were first identified genetically by their requirements for robust accumulation of *SUC2* mRNA (Tu *et al.* 1993; Yeghiayan *et al.* 1995; Kamura *et al.* 2001). The transcription factor Rim101 is proteolytically activated on recruitment to the MVB outer membrane via ESCRT-III factor Snf7/Vps32 to permit expression of pH-responsive genes (Boysen and Mitchell 2006). The Gα subunit (Gpa1) of a heterotrimeric G protein activates the PI 3-kinase Vps34 (a class D Vps factor) at the endosomal membrane to promote the transcriptional response to mating factors (Slessareva *et al.* 2006). Activation of genes for utilization of alternative nitrogen sources by Gln3 is enhanced by Vps factors, and it appears that Gln3 must traffic in vesicles containing Vps10 between Golgi and endosome for subsequent nuclear entry (Puria *et al.* 2008). Recently, evidence was presented that the phosphoinositide PI(3,5)P_2, produced at the late endosome promotes assembly of a transcriptional cofactor complex that enhances galactose induction of *GAL* gene transcription in the nucleus (Han and Emr 2011).

We found previously that robust activation of amino acid biosynthetic genes by yeast transcription factor Gcn4 requires a subset of Vps factors that function at the MVB. The defects in activation of Gcn4 target genes were most pronounced in mutants lacking certain Vps C or D factors, with lesser but still significant defects observed in *vps* mutants lacking particular ESCRT proteins, including ESCRT-II factors (Snf8/Vps22, Vps25, or Vps36) and ESCRT-III subunits Snf7/Vps32 and Vps20. Gcn4 synthesis is induced at the translational level in response to starvation for any single amino acid (Hinnebusch 2005). In the *vps* mutants, Gcn4 synthesis was induced properly and Gcn4 could enter the nucleus and bind to upstream activation sequences (UAS), but did not efficiently stimulate preinitiation complex (PIC) assembly at the promoter (Zhang *et al.* 2008). We hypothesized that a signal transduction pathway operates to dampen the transcriptional response to amino acid starvation by Gcn4 in response to endosome dysfunction (Zhang *et al.* 2008). More recently, evidence was provided that sterol limitation also down-regulates Gcn4 function in the nucleus, in a manner involving sterol binding protein Kes1 and its ability to inhibit PI(4)P-directed vesicular protein trafficking with an attendant increase in cellular sphingolipids. It appears that elevated sphingolipids provoke a reduction in Gcn4 function in a manner involving the CDK8 module of the transcriptional coactivator Mediator complex (Mousley *et al.* 2012).

In our previous study, some of the strongest defects in transcriptional activation by Gcn4 were observed in mutants lacking Vps34 and Vps15. Vps34 is the sole kinase in budding yeast that synthesizes PI(3)P in endomembranes, and Vps15 is a protein kinase associated with Vps34 required for its function (Bowers and Stevens 2005). Galactose induction of a *GAL1-lacZ* reporter was impaired in *vps15Δ* and *vps34Δ* mutants, but not as dramatically as seen for Gcn4-dependent reporters, suggesting that the function of Gal4, and possibly other transcriptional activators besides Gcn4, is also down-regulated to a lesser extent in response to endosome dysfunction. However, as shown below, we found subsequently that PIC assembly and transcription initiation occurs normally at the *GAL1* promoter in *vps15Δ* and *vps34Δ* mutants. Furthermore, *vps15Δ* and *vps34Δ* mutations evoked much stronger reductions in expression of *lacZ* reporters driven by Gcn4 compared to mRNA transcripts of authentic Gcn4 target genes (Zhang *et al.* 2008). These last observations led us to suspect that the greatly reduced expression of *lacZ* reporters observed in *vps* mutants involved a defect in transcription elongation in addition to the defective PIC assembly observed specficially for Gcn4 target genes. Indeed, it is well established by Aguilera and colleagues that efficient elongation through *lacZ* coding CDS requires a full complement of transcription elongation factors in yeast cells (Chavez *et al.* 2001; Morillo-Huesca *et al.* 2006)—a fact which has been exploited to identify novel factors involved in transcription elongation (Tous *et al.* 2011).

Accordingly, we set out to investigate whether Vps15, Vps34, and various other soluble Vps factors are required for efficient transcription elongation in yeast cells. The results presented below support this possibility, including evidence that the rate of elongation by Pol II through *lacZ* coding sequences is reduced in *vps15Δ* and *vps34Δ* cells. Our findings further suggest that reduced cotranscriptional recruitment of the histone acetyltransferase complex NuA4 to CDSs could be one factor underlying the elongation defect in these mutants. Interestingly, we also obtained evidence that elimination of Vps15 or Vps34 impairs localization of the *GAL1* and *INO1* genes to the nuclear periphery during transcriptional activation. Unexpectedly, using chromatin immunoprecipitation (ChIP) analysis, we detected cross-linking of these and several other Vps proteins to the CDSs of various genes *in vivo* in a manner dependent on transcriptional activation. Consistent with this, we detected dynamic association of a fraction of GFP-tagged Vps15 and Vps34 with nuclear pores in live cells under various culture conditions. Together, our results indicate that inactivation of various Vps proteins reduces the efficiency of transcription elongation *in vivo* and raise the possibility that at least a subset of these proteins might stimulate transcription elongation in a manner involving their physical association with, or proximity to, transcribed chromatin at the nuclear periphery.

Materials and Methods

Yeast strain and plasmid constructions

All strains and plasmids used in this study are listed in Tables 1 and 2, respectively. Wild-type (WT) strain BY4741 and deletion derivatives thereof were described previously (Giaever *et al.* 2002) and purchased from Research Genetics.

The presence of the reported deletion alleles was confirmed by PCR amplification of genomic DNA (Swanson *et al.* 2003). Strains harboring myc_{13} epitope tags were generated as described previously (Swanson *et al.* 2003) and verified by PCR analysis of chromosomal DNA and Western blot analysis with anti-myc antibodies. Strains harboring *trp1*Δ::*hisG* were generated using *TRP1* knock-out construct pNK1009 as described previously (Alani *et al.* 1987).

Strains CRY1605 and CRY1606 were generated by transformation of strains CRY1541 and CRY1581 with plasmid pNSP1-RFP. Strains HQY1584 and HQY1586 were constructed by transforming strains CRY1541 and CRY1581, respectively, with *Nur*I-digested pHQ2061, harboring the *SPT4-mCherry*::*hphMX4* cassette, selecting for growth on YPD containing hygromycin. Replacement of *SPT4* with *SPT4-mCherry*::*hphMX4* was confirmed by PCR analysis of chromosomal DNA using primers 972 and 1167 (Table 3), and by Western blot analysis using antibodies against mCherry.

NSP1 was tagged at its C terminus with *mTagBFP* in strains HQY1584 and HQY1587 to yield strains CRY1718 and CRY1719, respectively, using a newly constructed tagging plasmid (I. Malcova, unpublished results). The latter was produced by inserting a *Xho*I–*Bam*HI fragment containing the gene encoding yeast enhanced *mTagBFP* (*ytBFP*, a kind gift of Mads Kaern's laboratory at the University of Ottawa) into p*FA6a-natNT2*. The *ytBFP*::*natNT2* cassette was PCR amplified from the resulting tagging plasmid with primers Nsp1mbfp5 and Nsp1C2 using Phusion DNA polymerase (NEB) and used to transform HQY1584 and HQY1587 by selecting for growth on YPD medium containing nourseothricin (100 μg/ml, cloNat, Werner Bioagents, Jena). Correct integration of the cassette was verified by PCR analysis using primers Nsp1diaC and mTAGBFPrev, and the size of the protein fusion was checked by Western blot analysis using anti-tRFP antibody (Evrogen).

Plasmid pHQ2061 was constructed by PCR amplification from genomic DNA of a fragment containing the WT *SPT4* CDS flanked by *Hin*dIII/*Nru*I and *Bam*HI sites using primers 1853/1854 and inserted between the *Hin*dIII and *Bam*HI sites of pBS35 (fusing *SPT4* CDS in-frame to *mCherry* CDS); subsequently a fragment containing the *SPT4 3′-UTR* flanked by *Sac*I–*Nru*I and *Spe*I sites was PCR amplified from genomic DNA using primers 1855/1856 and inserted between the *Sac*I and *Spe*I sites of pBS35 to produce pHQ2061. Plasmid pNG18 was constructed by PCR amplification of an ~0.97-kb *URA3* fragment from genomic DNA of WT strain BY4741 by using primers N381/N382. The PCR-amplified *URA3* fragment was digested with *Bam*HI/*Cla*I and cloned into *Bam*HI/*Cla*I-digested *pCM184LAUR*.

Strains H1486 (wild type), NGY11 (*vps34*Δ), and NGY12 (*vps15*Δ) were transformed with GFP-Lac repressor plasmid pAFS144 digested with *Nhe*I (Straight *et al.* 1996). The resulting strains were transformed with either p6LacO128-GAL1 digested with *Nru*I (Brickner *et al.* 2007) or p6LacO128-INO1 digested with *Stu*I (Brickner and Walter 2004), giving rise to the following six strains: DBY375 (*GAL1*:*LacO*), DBY376 (*vps34*Δ *GAL1*:*LacO*), DBY377 (*vps15*Δ *GAL1*:*LacO*), DBY452 (*INO1*:*LacO*), DBY455 (*vps34*Δ *INO1*:*LacO*), and DBY457 (*vps15*Δ *INO1*:*LacO*).

Gene length-dependent accumulation of mRNA assays and Northern analysis

Measurement of Pho5 enzymatic activity for gene length-dependent accumulation of mRNA (GLAM) ratio determinations was carried out as described previously using transformants of the appropriate strains harboring plasmids YCplac33 (empty *URA3* vector), pSCH202 (P_{GAL1}-*PHO5*, *URA3*) and either pSCH209 (P_{GAL1}-*PHO5-LAC4*, *URA3*), or pSCH212 (P_{GAL1}-*PHO5-lacZ*, *URA3*) (Morillo-Huesca *et al.* 2006).

Isolation of total RNA from yeast and Northern blot analysis were carried out as described previously (Ginsburg *et al.* 2009). DNA probes used were a 0.9-kb *Eco*RV-digested *PHO5* internal fragment isolated from plasmid pSCH202, or the following PCR fragments amplified from the genomic DNA of BY4741 using primers listed in Table 3: 0.45 kb of *YAT1* CDS, 0.57 kb of *LYS2* CDS, 0.4 kb of *IMD2* CDS, and 0.9 kb of the *SCR1* gene. Each DNA fragment was radiolabeled with [α^{32}P]-dCTP by using the Megaprime DNA labeling system (Amersham).

Analysis of GAL1 positioning in yeast nuclei

Chromatin localization experiments were performed as described (Brickner *et al.* 2010) using strains expressing GFP fused to Lac repressor and the *GAL1* gene marked with an array of Lac repressor binding sites. Cells were stained with antibodies against GFP and Nsp1.

ChIP analysis

Yeast cell cultures (100 ml) at A_{600} of 0.5 to 0.6 were mixed with 11 ml of formaldehyde solution [50 mM HEPES-KOH (pH 7.5), 1 mM EDTA, 100 mM NaCl, and 11% formaldehyde] and cross-linked for 20 min at room temperature with intermittent shaking and then quenched with 15 ml 2.5 M glycine. Cells were collected by centrifugation and washed twice with 100 ml ice-cold Tris-buffered saline. The cells were broken by vortexing with glass beads in 500 μl of lysis buffer [50 mM HEPES-KOH (pH 7.5), 1 mM EDTA, 140 mM NaCl, 1% Triton X-100, 0.1% sodium deoxycholate, and protease inhibitors]. Glass beads were removed from the lysates and washed with 500 μl of lysis buffer, and the resulting 1-ml lysates were sonicated to yield DNA fragments of 300–500 bp. Supernatants containing soluble chromatin were obtained by centrifugation at 13,000 × *g* and stored at −80°. Fifty microliters of chromatin were used for immunoprecipitations, and an identical aliquot was reserved as the "input" sample. Chromatin was immunoprecipitated using Dynabeads Pan Mouse IgG (Invitrogen) coupled with antibodies described below for 2 hr at 4°, recovered immune complexes were washed once with phosphate-buffered saline (PBS) containing BSA (5 mg/ml), twice each with lysis buffer, wash-buffer I [50 mM HEPES-KOH (pH 7.5), 1 mM EDTA, 500 mM NaCl, 1% Triton X-100, and 0.1%

Table 1 Yeast strains used in this study

Name	Parent	Relevant genotype[a]	Reference
BY4741[b]	NA	*MATa his3Δ1 leu2Δ0 met15Δ0 ura3Δ*	Research Genetics
249[b]	BY4741[b]	*gcn4Δ::kanMX4*	Research Genetics
1044[b]	BY4741[b]	*gal4Δ::kanMX4*	Research Genetics
3236[b]	BY4741[b]	*vps15Δ::kanMX4*	Research Genetics
5149[b]	BY4741[b]	*vps34Δ::kanMX4*	Research Genetics
1580[b]	BY4741[b]	*snf7Δ::kanMX4*	Research Genetics
2826[b]	BY4741[b]	*snf8Δ::kanMX4*	Research Genetics
5381[b]	BY4741[b]	*vps27Δ::kanMX4*	Research Genetics
5588[b]	BY4741[b]	*vps4Δ::kanMX4*	Research Genetics
6986[b]	BY4741[b]	*spt4Δ::kanMX4*	Research Genetics
1764[b]	BY4741[b]	*thp1Δ::kanMX4*	Research Genetics
2861[b]	BY4741[b]	*thp2Δ::kanMX4*	Research Genetics
3682[b]	BY4741[b]	*pep7Δ::kanMX4*	Research Genetics
1812[b]	BY4741[b]	*pep12Δ::kanMX4*	Research Genetics
3043[b]	BY4741[b]	*vps10Δ::kanMX4*	Research Genetics
4462[b]	BY4741[b]	*vps45Δ::kanMX4*	Research Genetics
FZY610	BY4741[b]	*SNF7-myc$_{13}$::HIS3**	This study
FZY642	5588[b]	*SNF7-myc$_{13}$::HIS3* vps4Δ::kanMX4*	This study
FZY644	BY4741[b]	*SNF8-myc$_{13}$::HIS3**	This study
FZY657	5588[b]	*SNF8-myc$_{13}$::HIS3* vps4Δ::kanMX4*	This study
NGY26	BY4741[b]	*VPS15-myc$_{13}$::HIS3**	This study
NGY27	BY4741[b]	*VPS34-myc$_{13}$::HIS3**	This study
NGY28	249[b]	*VPS15-myc$_{13}$::HIS3* gcn4Δ::kanMX4*	This study
NGY29	249[b]	*VPS34-myc$_{13}$::HIS3* gcn4Δ::kanMX4*	This study
H3834/ HQY700	BY4741[b]	*arg1-ΔTATA*	(Qiu *et al.* 2006)
NGY56	H3834	*arg1-ΔTATA VPS15-myc$_{13}$::HIS3**	This study
NGY57	H3834	*arg1-ΔTATA VPS34-myc$_{13}$::HIS3**	This study
BY4705	NA	*MATα ade2Δ::hisG[c] his3-200Δ leu2Δ0 ura3Δ0 trp1-63Δ lys2Δ0met15Δ0*	(Liu *et al.* 2004)
SHY508A	BY4705	*kin28:kin28-as(L83G)* pSH579[*kin28-as(L83G) URA3 CEN*]	(Liu *et al.* 2004)
NGY68	BY4705	*VPS15-myc$_{13}$::HIS3**	This study
NGY69	BY4705	*VPS34-myc$_{13}$::HIS3**	This study
NGY102	3236[b]	*EPL1-myc$_{13}$::HIS3**	This study
NGY103	5149[b]	*EPL1-myc$_{13}$::HIS3**	This study
NGY117	BY4741[b]	*EPL1-myc$_{13}$::HIS3**	This study
NGY118	BY4741[b]	*YNG2-myc$_{13}$::HIS3**	This study
NGY119	3236[b]	*YNG2-myc$_{13}$::HIS3**	This study
NGY120	5149[b]	*YNG2-myc$_{13}$::HIS3**	This study
NGY98	BY4741[b]	*VPS27-myc$_{13}$::HIS3**	This study
NGY99	BY4741[b]	*VPS4-myc$_{13}$::HIS3**	This study
NGY100	BY4741[b]	*PEP7-myc$_{13}$::HIS3**	This study
NGY101	BY4741[b]	*VPS45-myc$_{13}$::HIS3**	This study
NGY116	BY4741[b]	*VPS10-myc$_{13}$::HIS3**	This study
H3881	BY4741[b]	*CDC33-myc$_{13}$::HIS3**	This study
H3879	BY4741[b]	*TIF32-myc$_{13}$::HIS3**	This study
NGY70	SHY508A	*kin28:kin28-as(L83G) VPS15-myc$_{13}$::HIS3** pSH579[*kin28-as(L83G) URA3 CEN*]	This study
NGY71	SHY508A	*kin28:kin28-as(L83G) VPS34-myc$_{13}$::HIS3** pSH579[*kin28-as(L83G) URA3 CEN*]	This study
NGY1	BY4741[b]	*trp1Δ::hisG[c]*	(Zhang *et al.* 2008)
NGY3	1580[b]	*snf7Δ::kanMX4 trp1Δ::hisG[c]*	(Zhang *et al.* 2008)
NGY4	3682[b]	*pep7Δ::kanMX4 trp1Δ::hisG[c]*	(Zhang *et al.* 2008)
NGY5	1812[b]	*pep12Δ::kanMX4 trp1Δ::hisG[c]*	(Zhang *et al.* 2008)
NGY6	3236[b]	*vps15Δ::kanMX4 trp1Δ::hisG[c]*	(Zhang *et al.* 2008)
NGY7	5149[b]	*vps34Δ::kanMX4 trp1Δ::hisG[c]*	(Zhang *et al.* 2008)
FZY810	5588[b]	*vps4Δ::kanMX4 trp1Δ::hisG[c]*	(Zhang *et al.* 2008)
CRY1541	BY4741	*MATα his3Δ1 leu2Δ0 met15Δ0 ura3Δ0 VPS34-GFP::HIS3MX6*	(Huh *et al.* 2003)
CRY1581	BY4741	*MATα his3Δ1 leu2Δ0 met15Δ0 ura3Δ0 VPS15-GFP::HIS3MX6*	(Huh *et al.* 2003)
CRY1605	CRY1541	*VPS34-GFP::HIS3MX6* pNSP1-RFP *[NSP1-RFP, URA3, CEN]*	This study
CRY1606	CRY1581	*VPS15-GFP::HIS3MX6* pNSP1-RFP *[NSP1-RFP, URA3, CEN]*	This study
HQY1584	CRY1541	*SPT4-mCherry::hphMX4, VPS34-GFP::HIS3MX*	This study
HQY1587	CRY1581	*SPT4-mCherry::hphMX4, VPS15-GFP::HIS3MX*	This study
CRY1718	HQY1584	*SPT4::mCherry::hphMX4 VPS34-GFP::HIS3MX NSP1-BFP::natNT2MX*	This study
CRY1719	HQY1587	*MATa SPT4-mCherry::hphMX4 VPS15-GFP::HIS3MX NSP1-BFP::natNT2MX*	This study
H1486	NA	*MATα his1-29 leu2-3, -112 ura3-52 ino1(?) <HIS4-lacZ, ura3-52>*	(Wek *et al.* 1992)

(continued)

Table 1, *continued*

Name	Parent	Relevant genotype[a]	Reference
NGY11	H1486	*vps34Δ::kanMX4*	(Zhang *et al.* 2008)
NGY12	H1486	*vps15Δ::kanMX4*	(Zhang *et al.* 2008)
DBY375	H1486	*GFP13-lacI-I12, lacO::GAL1*	This study
DBY376	NGY11	*GFP13-lacI-I12, lacO::GAL1 vps34Δ::kanMX4*	This study
DBY377	NGY12	*GFP13-lacI-I12, lacO::GAL1 vps15Δ::kanMX4*	This study
DBY452	H1486	*GFP13-lacI-I12, lacO::INO1*	This study
DBY455	NGY11	*GFP13-lacI-I12, lacO::INO1 vps34Δ::kanMX4*	This study
DBY457	NGY12	*GFP13-lacI-I12, lacO::INO1 vps15Δ::kanMX4*	This study
			This study

NA, not applicable.
[a] *HIS3** designates the *HIS3* allele from *S. kluyveri*.
[b] Purchased from Research Genetics.
[c] hisG: hisG sequences from *S. typhimurium*.

Na-deoxycholate] and wash-buffer II [10 mM Tris-HCl (pH 8.5), 250 mM LiCl, 1 mM EDTA, 0.5% NP-40, and 0.5% sodium deoxycholate], and once with TE [10 mM Tris-HCl (pH 8.0) and 1 mM EDTA]. The immunoprecipitated complexes were eluted at 65° for 15 min with 100 μl elution buffer [50 mM Tris-HCl (pH 8.0), 10 mM EDTA and 1% SDS] and for 10 min with 150 μl of elution wash buffer [50 mM Tris-HCl (pH 8.0), 1 mM EDTA, and 0.67% SDS], and the eluates were combined (IP sample). The matched input and IP samples were incubated overnight at 65° to reverse the cross-links. The samples were then treated with proteinase K (Ambion), at 100 μg/250 μl of chromatin, for 2 hr, and DNA was extracted twice with phenol:chloroform: isoamyl alcohol (25:24:1) and once with chloroform:isoamyl alcohol (24:1), ethanol precipitated, and resuspended in 30 μl TE containing RNase (10 μg/ml). Two microliters of resuspended DNA from IP and input samples were used for each PCR reaction in the presence of [^{33}P]-dATP with the appropriate primers (listed in Table 4). The radiolabeled amplified fragments were resolved by PAGE and quantified with a phosphorimager. For each primer set employed, we optimized the PCR conditions to ensure that the amounts of amplified ^{33}P-labeled products being generated are proportional to the amounts of input DNA over the range of DNA concentrations present in the IP or input samples. For the ChIP analysis of Snf7-myc and Snf8-myc in Figure 7, G–I, and of Rpb3 in Figure 3A, *POLI* CDSs were amplified as a negative control in addition to the specific *ARG1* or *GAL1* sequences of interest. An intergenic sequence from chromosome V (ChrV-1) was amplified as a negative control for all other ChIP experiments using primers 948/949, with the exception of the Rpb3 ChIP in Figure 4 where primers ExtChrV-1/ExtChrV-2 (ChrV-2) were used instead. Two immunoprecipitations were conducted on at least two chromatin samples isolated from independent cultures and the PCR analysis of IP and input DNA samples was carried out in duplicate or triplicate. Ratios of the amounts of PCR fragments for specific to control DNA sequences generated from IP samples were normalized to the corresponding ratios for input samples to yield occupancy values, and mean occupancies were calculated from replicate experiments.

Antibodies

Unless stated otherwise, 1 μl of the following antibodies was used for each ChIP assay: Mouse monoclonal anti-Rpb3 (Neoclone), mouse monoclonal anti-myc (Roche), and mouse anti-Ser5P-Rpb1 (H14 from Covance). For Western blot analysis of myc$_{13}$-tagged proteins in whole cell extracts prepared under denaturing conditions (Reid and Schatz 1982), the anti-myc antibody was used at the dilution recommended by the vendor.

Live-cell imaging by fluorescence microscopy

Distributions of fusion proteins in living cells were analyzed with an oil immersion 100×/1.4 objective using the Olympus Cell R detection and analyzing system based on the motorized Olympus IX-81 inverted microscope, Hammamatsu Orca/ER digital camera and the following highly specific mirror units: (i) EGFP filter block U-MGFPHQ, excitation (exc) max 488 nm, emission (em) max 507 nm; (ii) RFP filter block U-MFRFPHQ, exc max 558 nm, em max 583 nm; and (iii) BFP filter block U-MFBFPHQ, exc max 390 nm, em max 460 nm). The Cell R system enables us to obtain several optical sections through the cell. Images were processed, merged, and analyzed using Olympus Cell R, Imaris, National Institutes of Health ImageJ and Adobe CS5 software. Images from selected optical layers were presented.

Results

Elimination of Vps15 or Vps34 confers sensitivity to 6-azauracil and mycophenolic acid and dampens IMD2 induction by these inhibitors

The strong reductions in *lacZ* reporter expression observed in *vps15Δ* and *vps34Δ* mutants (Zhang *et al.* 2008) led us to suspect that the efficiency of transcription elongation was impaired in cells lacking these Vps proteins. To gain additional evidence for a transcription elongation defect, we examined sensitivity of *vps15Δ* and *vps34Δ* cells to the drugs 6-azauracil (6-AU) and mycophenolic acid (MPA). These drugs lower GTP pools by inhibiting IMP dehydrogenase

Table 2 Plasmids used in this study

Plasmid	Description	Source
pNK1009	*trp1Δ::hisG::URA3*, *TRP1* disruption plasmid	(Zhang *et al.* 2008)
YCplac33	*URA3*, *CEN4*	(Gietz and Sugino 1988)
pSCH202	P_{GAL1}-*PHO5*, *URA3*, *CEN6*	(Morillo-Huesca *et al.* 2006)
pSCH209	P_{GAL1}-*PHO5-LAC4*, *URA3*, *CEN6*	(Morillo-Huesca *et al.* 2006)
pSCH212	P_{GAL1}-*PHO5-lacZ*, *URA3*, *CEN6*	(Morillo-Huesca *et al.* 2006)
pSCH227	P_{GAL1}-*LYS2*, *URA3*, *CEN6*	(Chavez *et al.* 2001)
pSCH247	P_{GAL1}-*YAT1*, *URA3*, *CEN6*	(Chavez *et al.* 2001)
pCM184-LAUR	P_{tet}-*lacZ-URA3*, *TRP1*, *CEN4*	(Jimeno *et al.* 2002)
pNG18	P_{tet}-*URA3*, *TRP1*, *CEN4*	This study
YCplac111	*LEU2*, *CEN4*	(Gietz and Sugino 1988)
pNG9	*VPS15*, *LEU2*, *CEN4*	(Zhang *et al.* 2008)
pNG10	$vps15^{E200R}$, *LEU2*, *CEN4*	(Zhang *et al.* 2008)
pNG11	*VPS34*, *LEU2*, *CEN4*	(Zhang *et al.* 2008)
pNG12	$vps34^{N736K}$, *LEU2*, *CEN4*	(Zhang *et al.* 2008)
pVPS15	*VPS15*, *URA3*, *CEN6*	(Slessareva *et al.* 2006)
pVPS15^{E200R}	$vps15^{E200R}$, *URA3*, *CEN6*	(Slessareva *et al.* 2006)
pVPS34	*VPS34*, *URA3*, *CEN6*	(Slessareva *et al.* 2006)
pVPS34^{N736K}	$vps34^{N736K}$, *URA3*, *CEN6*	(Slessareva *et al.* 2006)
pNSP1-RFP	*NSP1-RFP*, *URA3*, *CEN4*	Kristine Willis
pBS35	*mCherry::hphMX4*	The Yeast Resource Center
pHQ2061	*SPT4-mCherry::hphMX4*	This study
pFA6a-natNT2	*natNT2*	(Janke *et al.* 2004)
NSP1-mTagBFP tagging plasmid	*NSP1-mTagBFP::natNT2*	This study
pAFS144	*GFP13-lacI-I12::HIS3*	(Straight *et al.* 1996)
p6LacO128-GAL1	*lacO::GAL1*	(Brickner *et al.* 2007)
p6LacO128-INO1	*lacO::INO1*	(Brickner *et al.* 2007)

(IMPDH) encoded by *IMD3* and *IMD4*, which catalyzes the rate-limiting step in *de novo* guanine nucleotide biosynthesis. Numerous mutations affecting transcription elongation factors confer sensitivity to both 6-AU and MPA (Exinger and Lacroute 1992; Jenks and Reines 2005 and references therein). Interestingly, *vps15Δ* and *vps34Δ* cells display sensitivity to these drugs comparable in degree to that exhibited by mutant cells lacking the elongation factor Spt4 (Hartzog *et al.* 1998), and these 6-AU-sensitive (6-AU^S) and MPA^S phenotypes were complemented by the corresponding WT *VPS* alleles on plasmids (Figure 1A). Significant, albeit reduced, sensitivity to MPA and 6-AU was also evident in the *pep7Δ/vps19Δ*, *pep12Δ/vps6Δ*, and *vps45*Δ mutants, and sensitivity to an even smaller degree was evident in the *vps4Δ* and *snf7Δ/vps32* strains as well (Figure 1, B and C). Like *vps15Δ* and *vps34Δ*, these other five *vps* mutants are also defective for vesicular protein transport from the Golgi to the vacuole (Bowers and Stevens 2005). Vps10 is an integral membrane protein that functions as the receptor for carboxypeptidase Y to mediate its trafficking from the late Golgi to late endosome (Bowers and Stevens 2005); and it was recently implicated in promoting nuclear entry of Gln3 (Puria *et al.* 2008); however, eliminating the *VPS10* gene conferred no sensitivity to 6-AU or MPA (Figure 1C).

Sensitivity to 6-AU and MPA does not necessarily indicate a transcription elongation defect; however, mutations in *bona fide* elongation factors have been found to reduce transcriptional induction of *IMD2*, encoding an MPA-resistant form of IMPDH (McPhillips *et al.* 2004), in response to 6-AU or MPA treatment (Riles *et al.* 2004). It is significant, therefore, that the *vps34Δ* mutation reduces *IMD2* mRNA abundance in the presence of 6-AU or MPA to an extent similar to that given by mutations that eliminate Spt4 or the Thp1 subunit of the elongation/mRNA export complex TREX-2 (Figure 1, D–G). Furthermore, complementation of the *IMD2* expression defect in *vps34Δ* cells by episomal *VPS34* was impaired by a mutation (*N736K*) that inactivates its PI 3-kinase activity (Slessareva *et al.* 2006) (Figure 1, D–G). These findings are consistent with the possibility that inactivation of the PI 3-kinase activity of Vps34 compromises the efficiency of transcription elongation *in vivo*.

Elimination of Vps15 or Vps34 impairs expression of lacZ reporters

We determined that *vps34Δ* and *vps15Δ* cells display another prominent phenotype of yeast elongation mutants, of inefficient elongation through the GC-rich or long CDS of bacterial *lacZ* and fungal *LAC4* (Chavez *et al.* 2001; Morillo-Huesca *et al.* 2006). First, we employed an *in vivo* reporter described by Aguilera and colleagues in which a *lacZ-URA3* translational fusion is expressed from the P_{tet} promoter in *ura3* auxotrophic strains. Mutations in known elongation factors impair expression of the *URA3* portion of the reporter and confer poor growth on (−Ura) medium lacking uracil (Jimeno *et al.* 2002). To control for possible effects of mutations on P_{tet} promoter activity, we constructed a matched P_{tet}-*URA3* reporter missing the *lacZ* CDS and compared growth of *vps* mutants harboring the P_{tet}-*lacZ-URA3* *vs.* P_{tet}-*URA3* reporters on −Ura medium. In the otherwise wild-type *ura3* strain, the P_{tet}-*lacZ-URA3* transformants grew

Table 3 Primers for strain construction or verification, or preparation of probes for Northern analysis

Name	Purpose	Sequence	Source
Kan B	Verification of *kanMX4* associated deletions	5′CTGCAGCGAGGAGCCGTAAT3′	(Winzeler *et al.* 1999)
Kan C	Verification of *kanMX4* associated deletions	5′TGATTTTGATGACGAGCGTAAT3′	(Winzeler *et al.* 1999)
FZP59	Reverse PCR primer to verify myc_{13} tags	5′AAATTCGCTTATTTAGAAGTGGCGC3′	This study
FZP136	Forward PCR primer to tag *SNF7* with myc_{13}	5′TGAAGGACGGGGAAGAGGAAGAGGATGAAGAAGATG AAGATGAAAAAGCATTAAGAGAACTACAAGCA GAAATGGGGCTTCGGATCCCCGGGTTAATTAA3′	This study
FZP137	Reverse PCR primer to tag *SNF7* with myc_{13}	5′GTATATAAAAGAGCGTATACAGAACATGGAAAGTAAGAA CACCTTTTTTTTTTCTTTCATCTAAACCGCATAGAACACGTG AATTCGAGCTCGTTTAAAC3′	This study
SNF7C	Forward PCR primer to verify *SNF7* myc_{13} tagging	5′GCAAGTCGAATTAGGAGATGAAATA3′	This study
N314	Forward PCR primer to tag *VPS15* with myc_{13}	5′ATTCTATATCTACATGTGAAGTTGATGAGACACCTTTGCTGG TTGCTTGTGATAACTCAGGGCTTATTGGAATCTTCCAACG GATCCCCGGGTTAATTAA3′	This study
N315	Reverse PCR primer to tag *VPS15* with myc_{13}	5′TGGTAAATGATCGAAAATGTTTAAGGTGAATACAAATTT ATACGCATTTAGAATAAAGAAGCTGAATAAAATAA AAAAAAGAATTCGAGCTCGTTTAAAC3′	This study
N316	Forward PCR primer to tag *VPS34* with myc_{13}	5′ATCTAATCAATGATAGTGTAAATGCTTTGCTGCCTATCG TGATTGATCATTTACATAATCTGGCACAATACTGGCGG ACCCGGATCCCCGGGTTAATTAA3′	This study
N317	Reverse PCR primer to tag *VPS34* with myc_{13}	5′ATATATTCAAGGTACCATTTATATGTTAAGTATAATTAGAG TGACGAAATTTAAATTTTGAAGCACCAATTATCAACCAA GAATTCGAGCTCGTTTAAAC3′	This study
N29	Forward PCR primer to verify *VPS15* myc_{13} tagging	5′TCAGTGACGTTTTTATTCCTACACA3′	This study
VPS34C	Forward PCR primer to verify *VPS34* myc_{13} tagging	5′TATTCGATTTTAAGAAGGAATGCAG3′	This study
N330/ N331	*IMD2* Northern probe	5′GTGGTATGTTGGCCGGTACTACCG3′ 5′TCAGTTATGTAAACGCTTTTCGTA3′	(Riles *et al.* 2004)
N332/ N333	*LYS2* Northern probe	5′TCAGTCCAATTAGGTAAGATTC3′ 5′AAGCTGCTGCGGAGCTTCCAC3′	This study
N334/ N335	*YAT1* Northern probe	5′AATTCAGCTCTTGCACGACGC3′ 5′CACGCTCACGTCGAAGTAATC3′	This study
SCR698/ SCR1699	*SCR1* Northern probe	5′CGCGGTACCTGATCAACTTAGCCAGGACATCC3′ 5′TGCTCTAGAGTTCTAAGTATTCTCATTTTATCC3′	(Qiu *et al.* 2004)
N381/ N382	*URA3* cloning for *pNG18* construction	5′GATCGGATCCATGTCGAAAGCTACATATAAGGA3′ 5′GATCATCGATTTAGTTTTGCTGGCCGCATCTT3′	This study
N394	Forward PCR primer to tag *YNG2* with myc_{13}	5′AAGAACCTCCGAAAGGAACATGGTACTGTCCCGAATGT AAAATTGAGATGGAAAAAAACAAACT GAAAAGAAAACGTAACCGGATCCCCGGGTTAATTAA3′	This study
N395	Reverse PCR primer to tag *YNG2* with myc_{13}	5′AGAATAGCAATCACCGTTTCTGGCTTATGGAATATT ATTAGTGTAAATGAGGTCATTCAGTCTCAAAAAGGT ATTTTTGTGAATTCGAGCTCGTTTAAAC3′	This study
N396	Forward PCR primer to verify *YNG2* myc_{13} tagging	5′AATGCGTTCTGGCGAACACTGC3′	This study
N362	Forward PCR primer to tag *VPS27* with myc_{13}	5′CACTTCCTGCAAGTTCCTCTGAAATTCCGATCAAAGAGGAAA GGCCGCCTAGTCCTCAAGAGGAACTGCTAATAGAGC TTCGGATCCCCGGGTTAATTAA3′	This study
N363	Reverse PCR primer to tag *VPS27* with myc_{13}	5′CAAGCAATTATATATATATGTATGTATATATTTATAAGCGCTA GGTTTCTTTTTACAAATACATAGAAAAGGCTACAATAGAA TTCGAGCTCGTTTAAAC3′	This study
N106	Forward PCR primer to verify *VPS27* myc_{13} tagging	5′TCCAGCAACTATCATCTCATCAATA3′	This study
N364	Forward PCR primer to tag *VPS4* with myc_{13}	5′AATCGACGAGACCTACCGTGAATGAGGATGACTTGCTGAA GCAAGAACAGTTCACTAGAGATTTTGGTCAAGAAGGTAA CCGGATCCCCGGGTTAATTAA3′	This study
N365	Reverse PCR primer to tag *VPS4* with myc_{13}	5′TAATTATTCTGTTTTTTTTTTTTTTTATTTTTTATTTTCATGTACAC AAGAAATCTACATTAGCACGTTAATCAATTGAGAATT CGAGCTCGTTTAAAC3′	This study

(continued)

Table 3, *continued*

Name	Purpose	Sequence	Source
N118	Forward PCR primer to verify *VPS4 myc$_{13}$* tagging	5′GCCAGGATAAAATGACTCAAAGTAA3′	This study
N377	Forward PCR primer to tag *PEP7* with *myc$_{13}$*	5′TCACACTTAATAAGAACTTAGAAGAATTGCACTCAAGAATA CATACCGTTCAATCGAAGCTGGGTGACCATGGGTTT AATCGGATCCCCGGGTTAATTAA3′	This study
N378	Reverse PCR primer to tag *PEP7* with *myc$_{13}$*	5′TACCCTTAAATAGATCTGATTGGCTCCGCGGACCAATTAGCG TGGAGATTCCGCGAATGATCGAATAATAAAGATATGT CGAATTCGAGCTCGTTTAAAC3′	This study
N308	Forward PCR primer to verify *PEP7 myc$_{13}$* tagging	5′TTGCTAAATATGATAGCATGCAAAA3′	This study
N379	Forward PCR primer to tag *VPS45* with *myc$_{13}$*	5′ATAACAGAATGAGGGTGGTTTTAGGAGGCACCTCTATACTTT CAACTAAAGAATATATGGATTCTATTAGATCTGCAAAA CGGATCCCCGGGTTAATTAA3′	This study
N380	Reverse PCR primer to tag *VPS45* with *myc$_{13}$*	5′ATGTTTTATCTGCATCGAAAAAGTTATATAGATTTATGCCTCATA TATAAAATAGAATTTTAGAATAAGATAATCCTTATGAATTCGA GCTCGTTTAAAC3′	This study
N118	Forward PCR primer to verify *PEP7 myc$_{13}$* tagging	5′GCCAGGATAAAATGACTCAAAGTAA3′	This study
N386	Forward PCR primer to tag *VPS10* with *myc$_{13}$*	5′ATGTTCCAGATACATTACCAGAAGGAAATGAGGAAAACATC GACAGGCCTGATTCTACAGCGCCATCTAACGAAAACC AGCGGATCCCCGGGTTAATTAA3′	This study
N387	Reverse PCR primer to tag *VPS10* with *myc$_{13}$*	5′TGATATTCTGTCTAAAGGATCTGCTCGTTTTTGTTTATGAAAA GTATATGGAATTATCTACTCTATGTAAAGTAATCTCTGAA TTCGAGCTCGTTTAAAC3′	This study
N114	Forward PCR primer to verify *VPS10 myc$_{13}$* tagging	5′AGGAAAAGAAAAAGAATTCAAGGAA3′	This study
FZP177	Forward PCR primer to tag *SNF8* with *myc$_{13}$*	5′CTAACGGTTTATTGTGGATTGATTATCAAGGTGGTGCAGAGG CGTTGTATTGGGATCCCTCTTGGATTACGAGGCAA CTGCGGATCCCCGGGTTAATTAA3′	This study
FZP178	Reverse PCR primer to tag *SNF8* with *myc$_{13}$*	5′CGGTAAGAACTGTGCTCAATAAAATACAACATCGATAAATAC TTAACGCTCATCCACCATTCCTGTTCAAGTCAACTATCG AATTCGAGCTCGTTTAAAC3′	This study
SNF8C	Forward PCR primer to verify *SNF8 myc$_{13}$* tagging	5′AGTAAATCTGCTCTTGATGAAATGG3′	This study
1853/1854	PCR amplification of the *SPT4* CDS for construction of pHQ2061	5′CGTACGAAGCTTTCGCGACGAGGTACAGTGTAA GAGATG3′/ 5′CCCGGGGATCCGCTCAACTTGACTGCCATCCCT3′	This study
1855/1856	PCR amplification of the *SPT4 3′UTR* for construction of pHQ2061	5′GAAAACGAGCTCTAAAACCTTCCGTTCTGATATC3′/ 5′TAGGCCACTAGTTCGCGACTGAGCTGCACGAGAAT3′	This study
972/1167	Verification of *SPT4-mCherry*::*hphMX* integration	5′CGTTCTATGAGTGAAATCGAG3′ 5′CAATTCAACGCGTCTGTGAG3′	This study
Nsp1mbfp5/ Nsp1C2	*ytBFP* cassette amplification	5′GATAACTCCACCTCTCTGGAAAAACAAATCAACTCGA TAAAGAAAGGTGCAGGTGCTGGAGCTGGT3′/ 5′CTATGTCAAATAAGTGTAGAATAGAGGGAATTTTTT CTTTTAGACACTATAGGGAGACCGGCAG3′	This study
Nsp1diaC/mTAGBFPrev	Verification of *ytBFP* cassette integration	5′GGTACTAGTGAAAGGAGGTG3′/ 5′CTACCTTCTAAACCACCGTC3′	This study
Epl1CMyc+	Forward PCR primer to tag *EPL1* with *myc$_{13}$*	5′GATTCGTTAATCAATTCAGAAGCGAAACAGAACTCTTCT ATAACCCAGAAAAATTCATCACGGATCCCCGGGTT AATTAA3′	This study
Epl1CMyc-	Reverse PCR primer to tag *EPL1* with *myc$_{13}$*	5′AGGTTTGTTAAATGCCAATGCGTAGAAAGATGTTCGAGAG GTACAAAGTTGTGCTGCTCAGAATTCGAGCTCGTTTAAAC3′	This study
N385	Forward PCR primer to verify *EPL1 myc$_{13}$* tagging	5′AGATGAACCGGCAAGACTTAAC3′	This study
mycCDC33F2	Forward PCR primer to tag *CDC33* with *myc$_{13}$*	5′ATTAACCGATGACGGGCATTTGGAATTCTTTCCACATTCC AGTGCCAATGGTAGACACCCTCAACCATCAATCACCTT GCGGATCCCCGGGTTAATTAA3′	This study
mycCDC33R1	Reverse PCR primer to tag *CDC33* with *myc$_{13}$*	5′GTATATATATTATATTATGATTATATATATAATTTTGATTAAA ATAACAATTATCTTAAGAAAAATTCAGACTATCGAATTCG AGCTCGTTTAAAC3′	This study

(continued)

Table 3, *continued*

Name	Purpose	Sequence	Source
mycTIF32F1	Forward PCR primer to tag *TIF32* with myc_{13}	5′CCCCAACTCCATCTTCTGGTCCAAAGAAAATGACTATGG CTGAAAAGTTGAGAGCCAAGAGATTGGCCAAGGGGGG CAGGCGGATCCCCGGGTTAATTAA3′	This study
mycTIF32R1	Reverse PCR primer to tag *TIF32* with myc_{13}	5′AATTGTTATTATGTACACATACTCTTATACGTATAAAAAA CGGTATAAATTAAGTAGATCATTTTGCGTTGTCTGGAA TTCGAGCTCGTTTAAAC3′	This study

more slowly and exhibited a lower plating efficiency, on SC −Ura compared to the corresponding P_{tet}-*URA3* transformants [Figure 2A, WT, *lacZ vs.* control (C)], indicating reduced expression of *URA3* CDS from the P_{tet}-*lacZ*-*URA3* reporter. The reduction in plating efficiency of P_{tet}-*lacZ*-*URA3 vs.* P_{tet}-*URA3* transformants was clearly exacerbated in the *vps15Δ*, *vps34Δ*, *pep7Δ*, and *pep12Δ* mutants, and possibly also in the *snf7Δ* strain, but not in the *vps4Δ* mutant (Figure 2A, SC −Ura, *cf*. *lacZ* and C transformants). These results, combined with the sensitivity of the *vps* mutants to 6-AU and MPA shown above, suggest that eliminating particular Vps proteins reduces the efficiency of transcription elongation, with relatively stronger defects conferred by the absence of Vps15 or Vps34 compared to other Vps factors, *e.g.*, Vps4, that are equally critical for vesicular protein transport to the vacuole.

To provide additional evidence for elongation defects in these *vps* mutants, we employed the GLAM assay developed by Morillo-Huesca *et al.* (2006) involving a P_{GAL1}-*PHO5*-*LAC4* construct harboring *LAC4* CDS inserted into the 3′-UTR and a matched P_{GAL1}-*PHO5* reporter with the same promoter but without *LAC4* CDS. The *LAC4* sequences add ∼3 kb to the transcript length but are not translated, such that both reporter transcripts produce the same Pho5 protein. A variety of mutants lacking known elongation factors express reduced steady-state amounts of the long reporter mRNA and, hence, decreased GLAM ratios of Pho5 enzyme activity produced from the long *vs.* short construct (Morillo-Huesca *et al.* 2006). In agreement with previous results for these reporters, the *spt4Δ* mutant exhibits a GLAM ratio that is only ∼20% of the WT value (Figure 2B). By comparison, the GLAM ratios in the *vps15Δ* and *vps34Δ* mutants were 50 and 40% of WT, and these defects were largely (*vps15Δ*) or completely (*vps34Δ*) complemented by the cognate WT alleles (Figure 2B).

We also conducted Northern analysis to quantify the GLAM ratios, and comparing mRNA expression from the P_{GAL1}-*PHO5*-*LAC4* and P_{GAL}-*PHO5* constructs revealed that deletions eliminating Spt4 or the Thp2 subunit of the Transcriptional defect of Hpr1 by Overexpression (THO) elongation complex (Chavez *et al.* 2000) confer strong reductions in the long/short mRNA ratio (Figure 2, C and D), as expected from previous results (Morillo-Huesca *et al.* 2006). Northern analysis of the *vps15Δ* and *vps34Δ* mutants confirmed the occurrence of ∼60% reductions in the ratio of long to short mRNAs produced by these two reporters and further revealed that complementation of these defects by the cognate plasmid-borne alleles was abolished by mutations that impair the protein kinase activity of Vps15 or PI 3-kinase activity of Vps34 (Slessareva *et al.* 2006) (Figure 2, C and D). Similar results were obtained using a P_{GAL1}-*PHO5*-*lacZ* reporter that contains *lacZ* instead of *LAC4* CDS in the 3′-UTR (Morillo-Huesca *et al.* 2006) (Figure 2, E and F). These findings support the conclusion that the efficiency of elongation is reduced in *vps15Δ* and *vps34Δ* cells, albeit not to the same extent observed in the known elongation mutants *spt4Δ* and *thp2Δ*.

The analyses of mRNA expression from the P_{GAL1}-*PHO5* constructs in the *vps15Δ* and *vps34Δ* mutants shown above suggested that these mutations do not significantly affect P_{GAL1} promoter activity (Figure 2, C and E, P_{GAL1}-*PHO5* blots), such that the reductions in expression of the long P_{GAL1}-*PHO5*-*LAC4* and P_{GAL1}-*PHO5*-*lacZ* reporters in these mutants likely involve defects in transcription elongation. To confirm that these *vps* mutations do not affect PIC assembly at the P_{GAL1} promoter, we conducted chromatin immunoprecipitation (ChIP) analysis of the Pol II subunit Rpb3 at the native *GAL1* promoter. As expected, elimination of the transcriptional activator Gal4 in the *gal4Δ* mutant reduces Rpb3 occupancy at the *GAL1* TATA box and CDS under galactose induction to the low, background levels observed in WT cells under noninducing conditions (Figure 3A). By contrast, the *vps15Δ* and *vps34Δ* mutants exhibit essentially WT levels of Rpb3 occupancy in the promoter region on galactose induction, confirming that PIC assembly is unaffected by elimination of the Vps15 and Vps34 proteins. A moderate reduction in Rpb3 occupancy in the CDS was observed in the *vps15Δ* strain, which would be consistent with a transcription elongation defect.

It has been shown that the long CDS of the native gene *LYS2* and the GC-rich CDS of *YAT1* exhibit enhanced requirements for elongation factors for efficient mRNA production (Chavez *et al.* 2001). To determine whether the *vps15Δ* and *vps34Δ* mutations also reduce the efficiency of transcription elongation through these native CDS, we examined mRNA expression from plasmid-borne P_{GAL1}-*YAT1* and P_{GAL1}-*LYS2* constructs harboring the *YAT1* or *LYS2* CDS. On induction with galactose, these constructs produce transcript levels far in excess of the endogenous *YAT1* or *LYS2* transcripts, and in a manner strongly dependent on the Hpr1 subunit of the THO elongation complex (Chavez *et al.* 2001) and Spt4 (Rondon *et al.* 2003a). As shown by

Table 4 Primers for ChIP assays

Name	Gene and location	Sequence	Source
273/274	*POL1* CDS	5′GACAAAATGAAGAAAATGCTGATGCACC-3′ 5′TAATAACCTTGGTAAAACACCCTG-3′	(Swanson *et al.* 2003)
605/ 607	*ARG1* UAS	5′ACGGCTCTCCAGTCATTTAT-3′ 5′GCAGTCATCAATCTGATCCA-3′	(Swanson *et al.* 2003)
265/266	*ARG1* TATA	5′TAATCTGAGCAGTTGCGAGA-3′ 5′ATGTTCCTTATCGCTGCACA-3′	(Qiu *et al.* 2004)
876/877	*ARG1* 5′ORF	5′TGGCTTATTCTGGTGGTTTAG-3′ 5′ATCCACACAAACGAACTTGCA-3′	(Qiu *et al.* 2004)
870/871	*ARG1* 3′ORF	5′CAGATCTATGATCCAACCATC-3′ 5′CTCATCCATAGAGGATTCTGT-3′	(Qiu *et al.* 2004)
UAS^{+}/UAS^{-}	*GAL1* UAS	5′CGCTTAACTGCTCATTGCTATATTG-3′ 5′TTGTTCGGAGCAGTGCGGCGC-3′	(Ginsburg *et al.* 2009)
TATA^{+}/TATA^{-}	*GAL1* TATA	5′AGTAACCTGGCCCCACAAAC-3′ 5′AAAGTGGTTATGCAGCTTTTCC-3	(Ginsburg *et al.* 2009)
5′ORF^{+}/5′ORF^{-}	*GAL1* 5′ORF	5′GCTGGGGTGGTTGTACTGTT-3′ 5′ATAGACAGCTGCCCAATGCT-3′	(Ginsburg *et al.* 2009)
mORF^{+}/mORF^{-}	*GAL1* mORF	5′TGCTCGATCCTTCTTTTCCA-3′ 5′TTGCGAACACCCTTGTTGTA-3′	(Govind *et al.* 2010)
3′ORF^{+}/3′ORF^{-}	*GAL1* 3′ORF	5′CGTTCATCAAGGCACCAAAT-3 5′TCAGAGGGCTAAGCATGTGT-3′	(Bryant and Ptashne 2003)
UAS1/UAS2	*ARG4* UAS	5′ GTTCTTGTGGTGGTTACTCA-3′ 5′ CCCTAGCTAAAGAAAGGTAG-3′	(QIU *et al.* 2004)
5′ORF1/5′ORF2	*ARG4* 5′ORF	5′AGATTCACTGGTGAAACCGAT-3′ 5′ACCTTCATGGATCTTTGCCAA-3′	(QIU *et al.* 2004)
3′ORF1/3′ORF2	*ARG4* 3′ORF	5′CCTTGGAGCAGTATCAAAAGA-3 5′CGTCGCCATCTGCTAATTTAA-3′	(QIU *et al.* 2004)
UAS1/UAS2	*ADH1* UAS	5′ATTCACGCACACTACTCTCTA-3′ 5′AACAAGGAAGAAAGGGAACGA-3′	(Govind *et al.* 2010)
3′ORF1/3′ORF2	*ADH1* 3′ORF	5′CTTACGTCGGTAACAGAGCTGA-3′ 5′ACCAACGATTTGACCCTTTTC-3′	(Govind *et al.* 2010)
5′ORF1/5′ORF2	*ADH1 5′ORF*	5′CCCACGGTMGTTGGAATA-3′ 5′TGACCACCGACTAATGGT-3′	This study
TATA1/TATA2	*PMA1* TATA	5′CGATTATATAAAAAGGCCAAATAT-3′ 5′TATCAACG AGGTTGATAGAAAAA-3′	(Qiu *et al.* 2004)
5′ORF1/5′ORF2	*PMA1* 5′ORF	5′CGACGACGAAGACAGTG ATA-3′ 5′ATTCTTTTTCGTCAGCCATTTG-3′	(Qiu *et al.* 2004)
3′ORF1/3′ORF2	*PMA1* 3′ORF	5′TGTTTTGGGTGGTTTCTACTACG-3′ 5′TTAGGTTTCCTTTTCGTGTTGAG-3′	(Qiu *et al.* 2004)
948/949	Intergenic ChrV (ChrV-1)	5′CCGATTTGTGAGATTCTTCCT-3′ 5′GAACAAGGTTACAAATCC TGAT-3′	(Qiu *et al.* 2004)
N376/ N352	P_{GAL1}-*PHO5-lacZ* -Promoter	5′CTGGGGTAATTAATCAGCGAAGCGATG-3′ 5′CGGCTAAAATTGAATAAACAACAG-3′	This study
N355/N356	P_{GAL1}-*PHO5-lacZ - lacZ1*	5′AAGAGGCCCGCACCGATCG-3′ 5′GGATAGGTTACGTTGGTGTAG-3′	This study
N357/N358	P_{GAL1}-*PHO5-lacZ - lacZ2*	5′GACACCACGGCCACCGATAT-3′ 5′CGCCAAGACTGTTACCCATC-3′	This study
N359/N360	P_{GAL1}-*PHO5-lacZ - lacZ3*	5′CAGCTGGCGCAGGTAGCAG-3′ 5′CCGTTTTCGCTCGGGAAGAC-3′	This study
ExtChrV-1/Ext ChrV-2	Intergenic ChrV-2	5′CATTTGCAATTTGCAGTTCAAC-3′ 5′TCAAATTGGGTGGAAAATGAAC-3′	This study

the Northern analyses in Figure 3, B and C, the *vps15Δ* and *vps34Δ* mutations reduce mRNA production from the P_{GAL1}-*YAT1* and P_{GAL1}-*LYS2* constructs by 40–60%, comparable to that given by the *spt4Δ* and *thp2Δ* mutations for the P_{GAL1}-*LYS2* construct, but much less than that observed for the P_{GAL1}-*YAT1* construct in *spt4Δ* cells.

As shown above, deletions of various *VPS* genes besides *VPS15* and *VPS34* conferred sensitivity to 6-AU and MPA (Figure 1, A–C) and also appeared to reduce transcription elongation through the P_{tet}-*lacZ-URA3* reporter (Figure 2A), albeit to lesser extents than observed in *vps15Δ* and *vps34Δ* cells. Hence, we characterized additional *vps* mutants in the GLAM assay using the P_{GAL1}-*PHO5-LAC4* and P_{GAL1}-*PHO5* constructs described above. With the exception of the *vps10Δ* and *snf7Δ* deletions, all of the *VPS* deletions we tested reduce the GLAM ratio significantly, but to different extents. Among the defective mutants, the *snf8Δ/vps22Δ* strain exhibits the smallest effect, reducing the ratio by only 21%, whereas

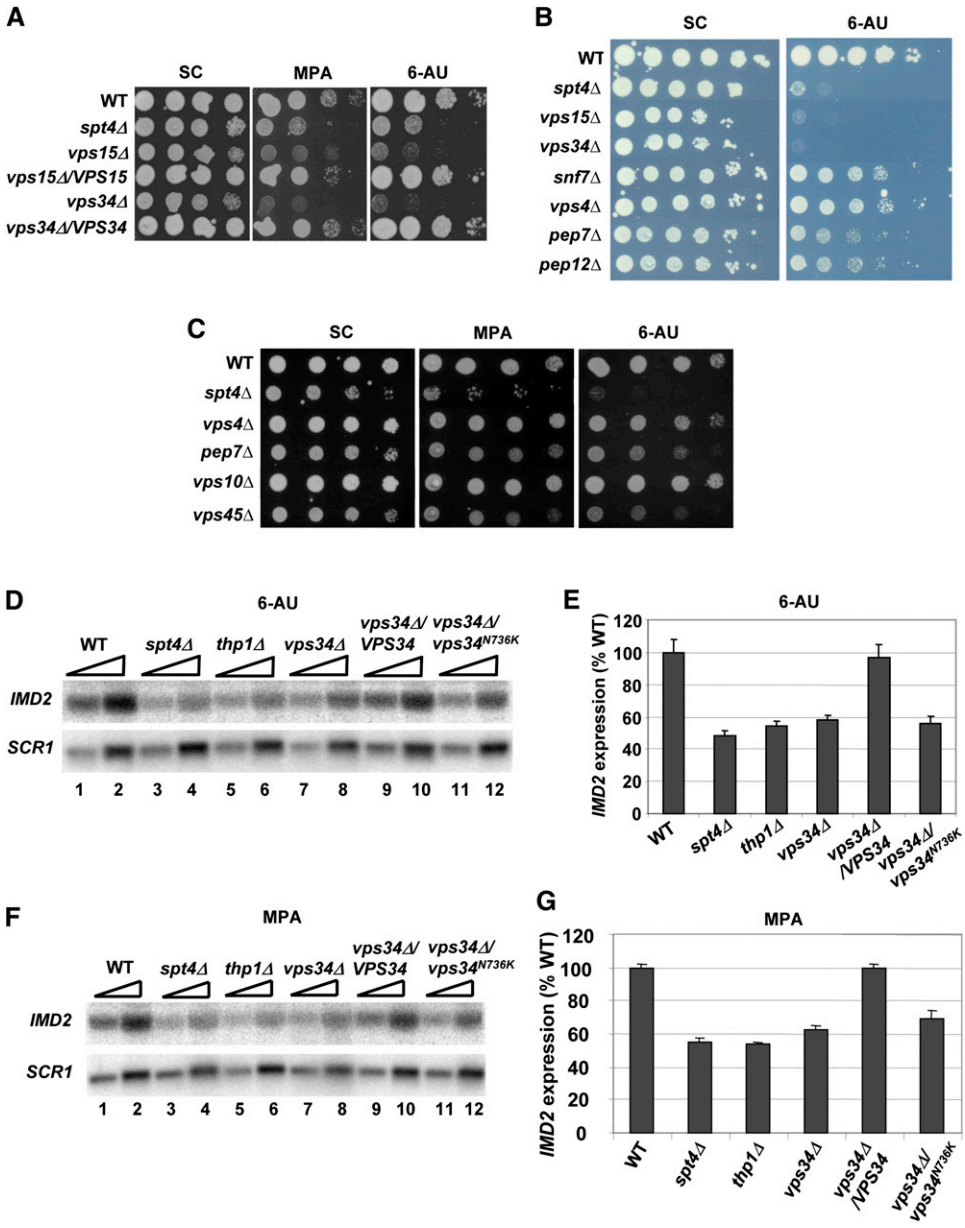

Figure 1 Vps factors are required for WT resistance to 6-AU and MPA and for robust induction of *IMD2* transcription by these elongation inhibitors. (A) Serial 10-fold dilutions of transformants of the indicated genotypes harboring an empty *URA3* vector (YCplac33) or *URA3* plasmids containing *VPS15* (p*VPS15*; row 4) or *VPS34* (p*VPS34*; row 6) spotted on SC −Ura or SC −Ura containing 15 μM MPA or 100 μg/ml 6-AU and incubated for 3 days (SC) or 5 days (MPA and 6-AU) at 30 °C. Transformants of WT (BY4741), *spt4Δ* (6986), *vps15Δ* (3236), and *vps34Δ* (5149) strains were analyzed. (B and C) Conducted as in A using transformants of WT (BY4741), *spt4Δ* (6986), *vps15Δ* (3236), *vps34Δ* (5149), *snf7Δ* (1580), *vps4Δ* (5588), *pep7Δ* (3682), *pep12Δ* (1812), *vps10Δ* (3043), and *vps45Δ* (4462) strains except that cells were incubated for 6 days on plates containing 75 μg/ml 6-AU. (D and E) Northern analysis of *IMD2* and *SCR1* transcripts in strains of the indicated genotypes cultured to mid-exponential phase in SC −Ura at 30 °C and incubated with 6-AU at 100 μg/ml for 2 hr. Total RNA was extracted and subjected to blot-hybridization analysis with probes for *IMD2* and *SCR1* transcripts. A representative blot is shown in D, in which successive lanes for each strain contain amounts of the same RNA samples differing by a factor of 2 (indicated by the ramps), and the mean ratios of *IMD2* to *SCR1* intensities quantified by phosphorimaging analysis of multiple experiments are plotted in E with the SEM shown as error bars. Empty vector transformants of WT (BY4741, lanes 1 and 2), *spt4Δ* (6986, lanes 3 and 4), *thp1Δ* (1764, lanes 5 and 6), and *vps34Δ* (5149, lanes 7 and 8) strains, a p*VPS34* transformant of strain 5149 (lanes 9 and 10), and a p*VPS34*^{N736K} transformant of strain 5149 (lanes 11 and 12) were analyzed. (F and G) Same as D and E except, using 15 μM MPA instead of 6-AU.

vps4Δ and *pep7Δ* decrease the ratio by ~40%. Consistent with its lack of 6-AU and MPA sensitivity (Figure 1C), the *vps10*Δ mutant displays a WT GLAM ratio (Figure 3D). Although the *vps15Δ* and *vps34Δ* mutants display the strongest reductions in the GLAM ratio among the *vps* mutants tested, a defect in elongation is exhibited to different extents by other *vps* mutants using *LAC4* (Figure 3D) and *lacZ* reporters (Figure 2A). However, because Snf7, Snf8, and Vps4 are required for vesicular protein trafficking from the MVB to vacuole, it appears that disruption of this process *per se* is not sufficient to confer the relatively stronger elongation defects displayed by *vps15Δ* and *vps34Δ* mutants.

Vps15 and Vps34 stimulate the rate of Pol II elongation through lacZ coding sequences in vivo

To gain further insight into the nature of the elongation defect displayed by the *vps15Δ* and *vps34Δ* mutants, we explored whether eliminating Vps15 or Vps34 reduces the rate of transcription elongation *in vivo*. To this end, we analyzed the kinetics of Pol II elongation through the *lacZ* coding sequences of the P_{GAL1}-*PHO5*-*lacZ* reporter. On glucose addition to cells growing with galactose, Pol II recruitment to the *GAL1* promoter is blocked and preexisting elongating Pol II molecules finish transcribing the CDS.

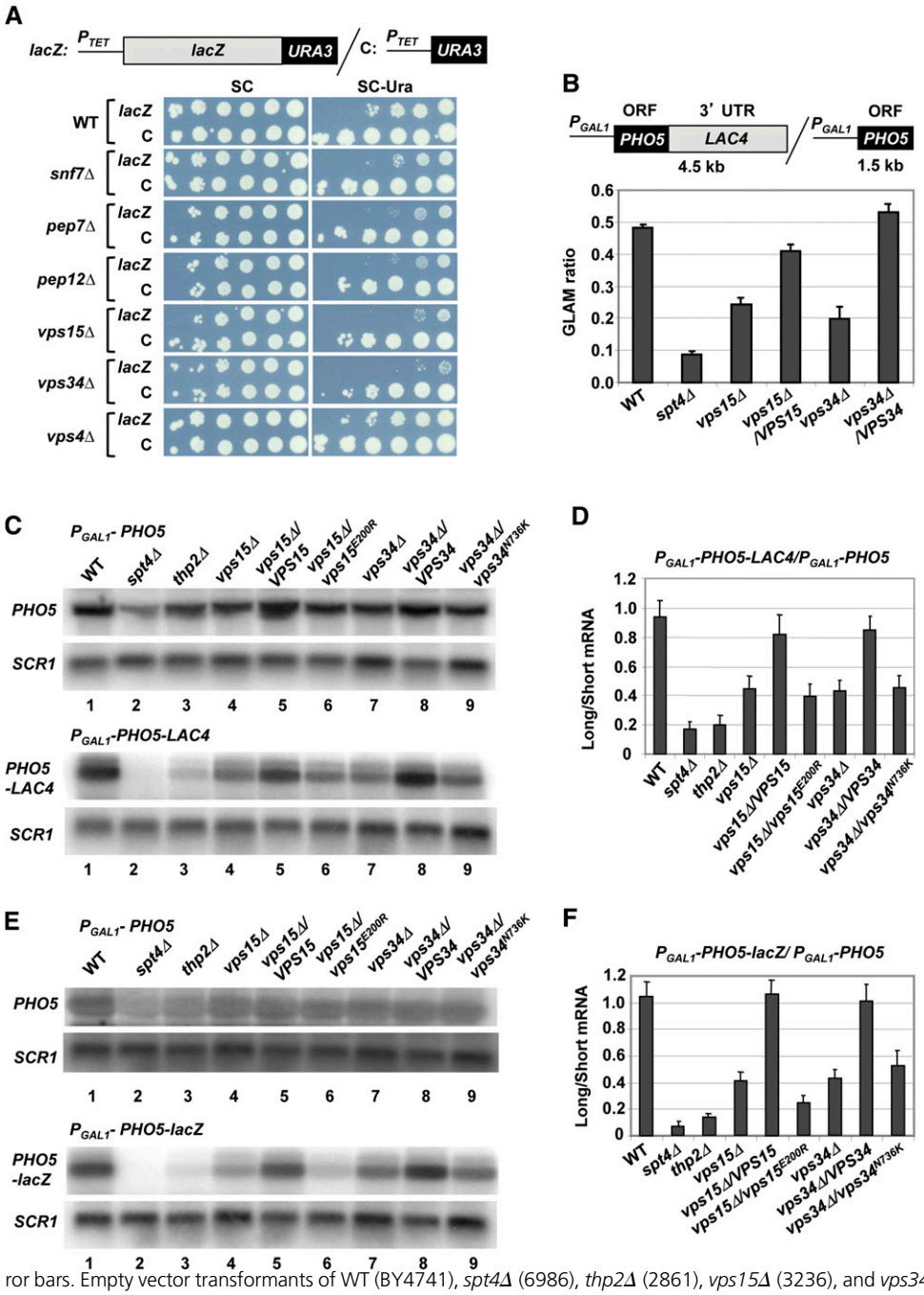

Figure 2 Vps factors are required for efficient transcription elongation through long and GC-rich coding sequences. (A) Serial 10-fold dilutions of transformants of the indicated genotypes harboring pCM184-*LAUR* (*lacZ*) containing P_{tet}-*lacZ-URA3* or control plasmid pNG18 (C) containing P_{tet}-*URA3* spotted on SC −Leu or SC −Leu −Ura and incubated for 5 days at 30 °C. The P_{tet}-*lacZ-URA3* and P_{tet}-*URA3* constructs are depicted schematically at the top. Transformants of WT (NGY1), *snf7Δ* (NGY3), *pep7Δ* (NGY4), *pep12Δ* (NGY5), *vps15Δ* (NGY6), *vps34Δ* (NGY7), and *vps4Δ* (FZY810) strains were analyzed. (B) Ratios of Pho5 enzymatic specific activity in transformants of the indicated genotypes harboring plasmids containing P_{GAL1}::*PHO5-LAC4* (pSCH209) or P_{GAL1}-*PHO5* (pSCH202) (both shown schematically above), *i.e.*, GLAM ratios, were measured. Strains also contained either empty *LEU2* vector YCplac111 (lanes 1–3 and 5) or plasmids containing *VPS15* (pNG9, lane 4) or *VPS34* (pNG11, lane 6). The appropriate transformants of WT (BY4741), *spt4Δ* (6986), *vps15Δ* (3236), or *vps34Δ* (5149) strains were grown to mid-exponential phase in SC −Ura −Leu with 2% galactose as carbon source at 30 °C before measuring Pho5 activity in whole cell extracts (WCE). (C and D) Northern analysis of transcripts from P_{GAL1}-*PHO5* (top two panels) and P_{GAL1}-*PHO5-LAC4* (bottom two panels) in strains of the indicated genotype grown to mid-exponential phase in SC −Ura −Leu containing 2% galactose as carbon source at 30 °C. Total RNA was extracted and subjected to blot-hybridization analysis with probes for the *PHO5* CDS or *SCR1*. A representative blot is shown in C and the mean ratios of *PHO5-LAC4* (long) to *PHO5* (short) mRNA levels, each normalized to *SCR1*, was quantified by phosphorimaging analysis of multiple experiments and plotted in D with the SEM shown as error bars. Empty vector transformants of WT (BY4741), *spt4Δ* (6986), *thp2Δ* (2861), *vps15Δ* (3236), and *vps34Δ* (5149) strains (lanes 1–4 and 7), a pNG9 transformant of strain 3236 (lane 5), a pNG10 transformant of strain 3236 (lane 6), a pNG11 transformant of strain 5149 (lane 8), and a pNG12 transformant of strain 5149 (lane 9) were analyzed. (E and F) Same as in C and D except that P_{GAL1}-*PHO5-lacZ* (pSCH212) was analyzed instead of P_{GAL1}-*PHO5-LAC4*.

The kinetics of Pol II run-off during this last wave of elongation can be determined by ChIP analysis of Rpb3 occupancy at various times after adding glucose, providing a measure of the elongation rate *in vivo* (Mason and Struhl 2005).

As expected, after addition of glucose to WT cells, Pol II vacated the promoter and 5′ end of the P_{GAL1}-*PHO5-lacZ* CDS more rapidly than from the 3′ end of the CDS. Thus, after 2 min, there was a large decline in Rpb3 occupancy at the promoter, progressively smaller reductions at locations 1.52 kb and 2.87 kb downstream from the promoter, and no reduction 4.06 kb from the promoter, whereas by 3 to 4 min, most of the Pol II had cleared the entire *lacZ* CDS (Figure 4B). Interestingly, the rate of Pol II run-off was significantly lower in the *vps15Δ* and *vps34Δ* mutants. This point is appreciated by noting that the decreases in Rpb3 occupancies at the 2.87-kb and 4.06-kb locations between 2 and 3 min in glucose in the mutant cells (Figure 4, C and D) were

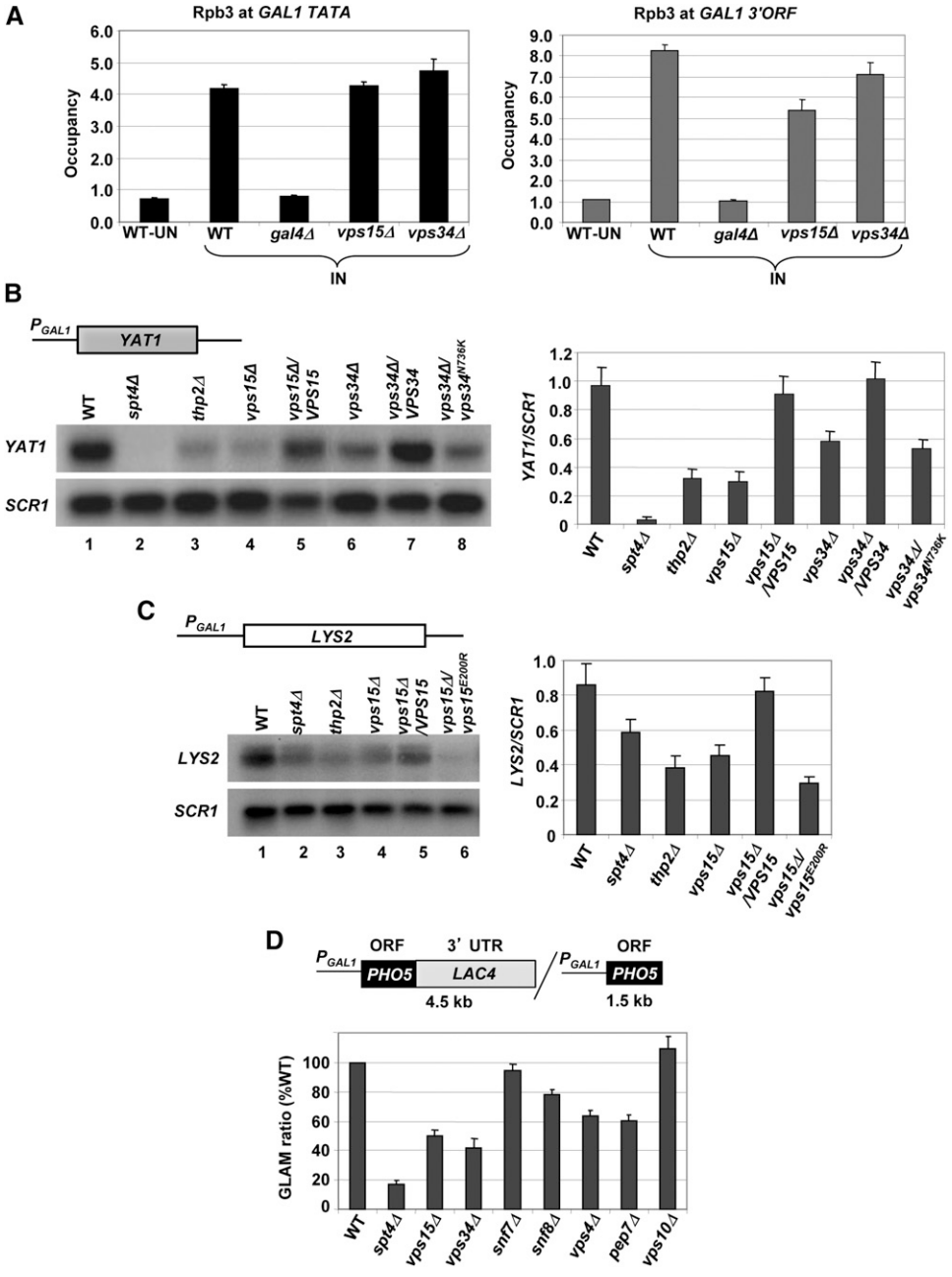

Figure 3 Vps factors do not affect PIC assembly at *GAL1* but are required for efficient transcription of several P_{GAL1}-driven CDS. (A) Occupancies of Rpb3 at the *TATA* region in the promoter and *3′ORF* of chromosomal *GAL1* were measured by ChIP analysis of strains of the indicated genotype cultured in SC medium containing 2% raffinose and either induced by adding galactose to 2% for 30 min (IN) or kept untreated (UI). Cross-linked chromatin was immunoprecipitated with anti-Rpb3 antibodies and DNA from immunoprecipitated (IP) and input samples was subjected to PCR (using primers listed in Table 4) in the presence of [^{33}P]-dATP to amplify radiolabeled fragments of the *GAL1 TATA* region, *3′ORF* , or *POL1 CDS* (Table 4) analyzed as a control, and the PCR amplicons were quantified by phosphorimaging analysis. Ratios of *GAL1 TATA* and *3′ORF* to *POL1 CDS* signals for IP samples were normalized to the corresponding ratios for input samples to yield occupancy values. Immunoprecipitations were conducted in duplicate on at least two chromatin samples prepared from two replicate cultures and the PCR analysis of precipitated DNA sequences was conducted in duplicate for each immunoprecipitated sample. Error bars represent the standard error of the mean (SEM). WT (BY4741), *gal4Δ* (1044), *vps15Δ* (3236), and *vps34Δ* (5149) strains were analyzed. (B) Northern analysis of transcripts expressed from P_{GAL1}-*YAT1* (shown schematically and contained on pSCH247) in strains of the indicated genotypes grown at 30 °C to mid-exponential phase in SC −Ura −Leu containing 2% raffinose and induced with 2% galactose for 2 hr. Total RNA was extracted and subjected to blot-hybridization analysis with probes to the *YAT1* CDS or *SCR1*. A representative blot is shown on the left and the mean ratios of *YAT1* mRNA to *SCR1* RNA levels were quantified by phosphorimaging analysis of multiple experiments and plotted here with the SEM shown as error bars. Empty vector transformants of WT (BY4741), *spt4Δ* (6986), *thp2Δ* (2861), *vps15Δ* (3236), and *vps34Δ* (5149) strains (lanes 1–4 and 6), a pNG9 transformant of strain 3236 (lane 5), a pNG11 transformant of strain 5149 (lane 7), and a pNG12 transformant of strain 5149 (lane 8), all harboring pSCH247, were analyzed. (C) Northern analysis of transcripts from P_{GAL1}-*LYS2* in strains of the indicated genotype conducted as in B except that the strains harbored pSCH227 *vs.* pSCH247, a pNG10 transformant of strain 3236 (lane 6) was analyzed, and probes of *LYS2* CDS and *SCR1* were employed. (D) GLAM ratios were measured as in Figure 2B using the appropriate transformants of WT (BY4741), *spt4Δ* (6986), *vps15Δ* (3236), *vps34Δ* (5149), *snf7Δ* (1580), *snf8Δ* (2826), *vps4Δ* (5588), *pep7Δ* (3682), and *vps10Δ* (3043) strains, harboring pSCH202 or pSCH209, and normalized to the GLAM ratio of the WT strain.

considerably smaller than the reductions observed between 2 and 3 min at the corresponding locations in WT cells (Figure 4B). Even after 5 min, the Pol II run-off was incomplete in both *vps* mutants (Figure 4, C and D). These findings suggest that elimination of Vps15 or Vps34 evokes a reduced rate of elongation by Pol II through the GC-rich *lacZ* CDS. The fact that in *vps15*Δ cells the Rpb3 occupancies were actually higher at the 3′ end of the CDS after 2 min in glucose than in galactose medium (Figure 4C) might indicate that the elongation defect in this mutant is exacerbated by the switch from galactose to glucose, leading to a modest build-up of Pol II toward the 3′ end of the CDS. Finally, ChIP analysis of Rpb3 occupancies across the *lacZ* CDS under steady-state inducing conditions (exponential growth in galactose medium), revealed no reductions in Pol II occupancy at the 3′ end relative to the 5′ end of the CDS in the *vps15Δ*

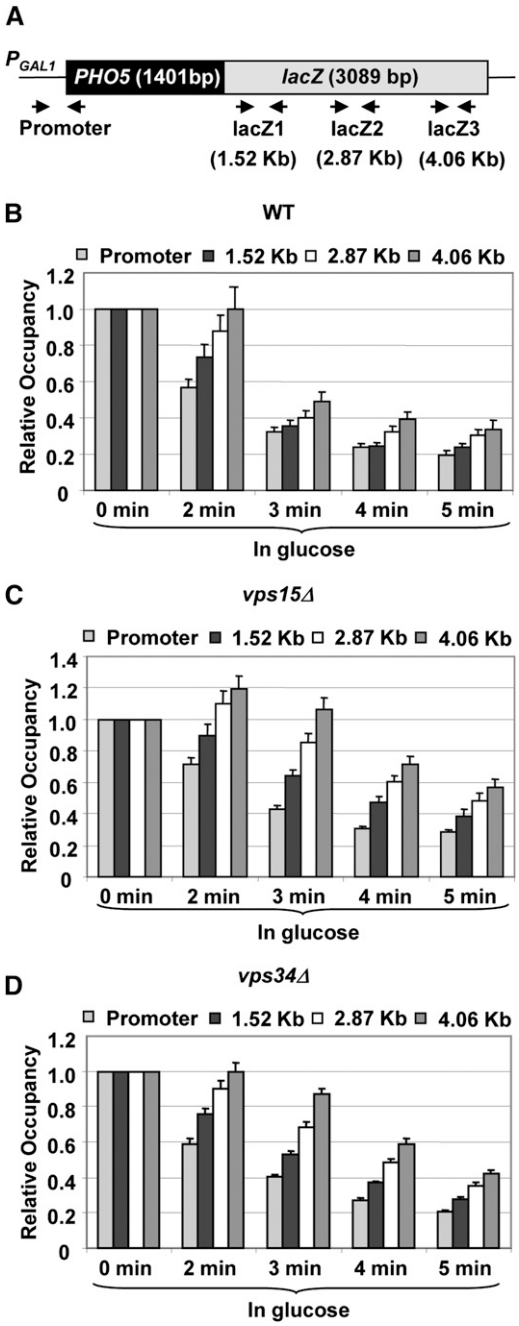

Figure 4 *vps15Δ* and *vps34Δ* mutations reduce the transcription elongation rate through *lacZ* CDS *in vivo*. (A–D) ChIP analysis of Pol II (Rpb3) occupancies across the P_{GAL1}-*PHO5-lacZ* construct. pSCH212 transformants of WT (BY4741) (B), *vps15Δ* (3236) (C), or *vps34Δ* (5149) (D) strains were grown in SC medium containing 2% raffinose at 30 °C, induced by adding galactose to 2% for 1 hr, and repressed by adding glucose to 4% for the indicated times (minutes) before cross-linking. ChIP was performed with anti-Rpb3 antibodies and PCR amplification in the presence of [α^{33}P]-dATP using the primers shown schematically in A, and listed in Table 4, located in the P_{GAL1} promoter or in *lacZ* CDS at the indicated distances downstream of the transcription start site, and the control ChrV-2 primers (that amplify an intergenic region on chromosome V). Rpb3 occupancies were calculated as described in Figure 3A, and the occupancies in glucose (2–5 min) were normalized to those in galactose (0 min) and set to unity for time zero. Mean relative occupancies and SEM (error bars) were calculated from immunoprecipitations conducted in duplicate on at least two chromatin samples prepared from two replicate cultures and the PCR analysis of precipitated DNA sequences was conducted in duplicate for each immunoprecipitated sample.

and *vps34Δ* mutants compared to the Pol II occupancies seen at the corresponding locations in WT cells (data not shown). Thus, elimination of these Vps factors does not seem to provoke dissociation of Pol II from the template DNA despite a reduction in the elongation rate during transcription of the *lacZ* CDS.

Cotranscriptional recruitment of NuA4 to CDS in vivo

A genome-wide study of genes directly involved in histone acetylation or deacetylation revealed an unexpected enrichment of genetic interactions with genes involved in endosome/vacuole functions. In particular, *vps15* and *vps34* mutations were found to be synthetically lethal with a mutation in Epl1, a subunit of the histone acetyltransferase (HAT) complex NuA4, and a *snf8* mutation was synthetically lethal with mutations in the Yng2 and Esa1 subunits of NuA4 (Lin *et al.* 2008). We recently presented evidence that NuA4 is cotranscriptionally recruited to CDS and that a conditional mutation affecting Esa1, the HAT catalytic subunit of NuA4, reduces the rate of Pol II elongation *in vivo* (Ginsburg *et al.* 2009). These findings led us to consider whether eliminating the Vps15 or Vps34 proteins from cells would reduce NuA4 recruitment to CDS as one aspect of the impairment of transcription elongation in *vps15Δ* and *vps34Δ* cells. To this end, we conducted ChIP analysis of a functional Myc-tagged version of the NuA4 subunit Epl1 at the *GAL1* gene. In agreement with previous results (Ginsburg *et al.* 2009), induction of *GAL1* with galactose leads to increased Myc-Epl1 occupancy of both the 5′ and 3′ ends of the *GAL1* CDS [Figure 5B, *cf*. WT uninduced (UI) *vs.* WT induced (IN)]. Interestingly, the Myc-Epl1 occupancy under inducing conditions is reduced at both locations in the *GAL1* CDS in *vps34Δ* cells to nearly the same levels seen in WT cells under noninducing conditions. In addition, the *vps15Δ* mutation reduces the galactose induction of Myc-Epl1 at the 3′ end of the *GAL1* CDS. Highly similar results were observed in ChIP analysis of Myc-Yng2, another subunit of NuA4 (Figure 5C). As shown above in Figure 3A, Rpb3 occupancy in the 3′ end of the *GAL1* CDS was reduced somewhat in these strains. However, the small reduction in Pol II occupancy clearly cannot account for the strong decrease in NuA4 occupancy seen in *vps34Δ* cells, and the reduction for NuA4 exceeds that of Pol II even in *vps15Δ* cells. Thus, we conclude that cotranscriptional recruitment of NuA4 to *GAL1* CDS is greatly compromised in cells lacking Vps34 and is also significantly impaired in the absence of Vps15.

Localization of activated GAL1 and INO1 at the nuclear periphery requires Vps15 and Vps34

The *GAL1* gene, when transcriptionally active, localizes at the nuclear periphery in association with the nuclear pore

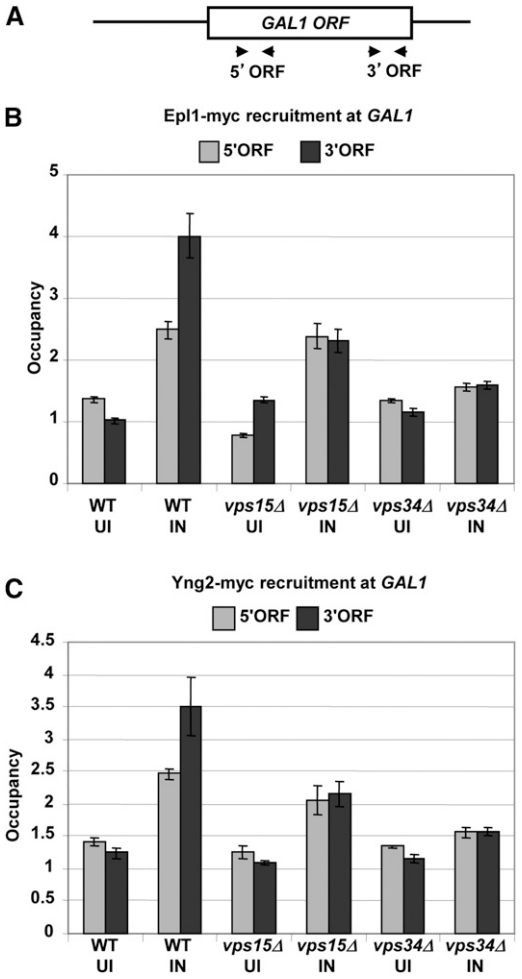

Figure 5 *vps15Δ* and *vps34Δ* mutations reduce cotranscriptional recruitment of NuA4. (A–C) ChIP analysis of myc-tagged NuA4 subunits Epl1 (B) and Yng2 (C) at *GAL1* CDS using primers depicted in A. In B, WT (NGY117), *vps15Δ* (NGY102), and *vps34Δ* (NGY103) strains, harboring *EPL1-myc*$_{13}$, were grown in SC medium containing 2% raffinose at 30 °C (UI), and induced with 2% galactose (IN) for 30 min before cross-linking. ChIP analysis was performed as described in Figure 3A except using anti-myc antibodies and the *GAL1* CDS primers depicted in A and control ChrV-1 primers (that amplify an intergenic region on chromosome V) listed in Table 4. In C, ChIP was performed as in B except using the following *YNG2-myc*$_{13}$ strains: WT (NGY118), *vps15Δ* (NGY119), and *vps34Δ* (NGY120). Immunoprecipitations were conducted in duplicate on at least two chromatin samples prepared from two replicate cultures and the PCR analysis of precipitated DNA sequences was conducted in duplicate for each immunoprecipitated sample. Error bars represent the standard error of the mean (SEM).

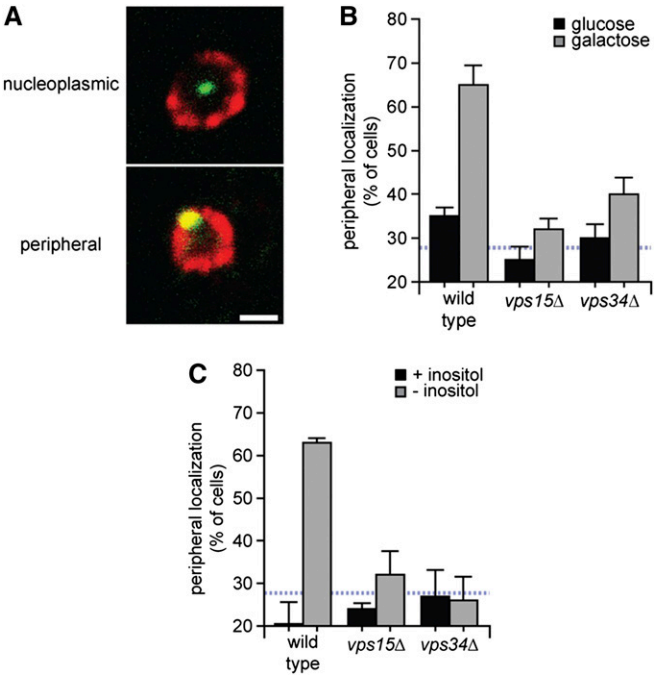

Figure 6 Localization of activated *GAL1* at the nuclear periphery requires Vps15 and Vps34. Strains DBY375 (WT), DBY376 (*vps34*Δ), and DBY377 (*vps15*Δ), containing an array of Lac repressor binding sites integrated at *GAL1* and expressing a GFP fusion to Lac repressor, were grown overnight in glucose-containing medium and then shifted to galactose medium for 2 hr before fixing in methanol and processing for immunofluorescence using antibodies against GFP-Lac repressor and Nsp1. (A) Representative cells stained for GFP (green) and Nsp1 (red) that were scored as nucleoplasmic or peripheral. (B) Average peripheral localization of *GAL1* from three biological replicates. For each replicate, ≥30 cells were counted. The mean percentage of cells in which the Lac repressor dot colocalized with the nuclear envelope (Nsp1) is displayed ±SEM. The dynamic range of this assay is from 20 to 80%, and the hatched line represents the distribution of the *URA3* gene with respect to the nuclear envelope. (C) Strains DBY452 (WT), DBY455 (*vps34*Δ), and DBY457 (*vps15*Δ), harboring an array of Lac repressor binding sites integrated at *INO1* and expressing GFP-tagged Lac repressor were cultured overnight in SC lacking inositol either containing or lacking 100 μM *myo*-inositol and analyzed as in B.

complex (Casolari *et al.* 2004; Cabal *et al.* 2006; Brickner *et al.* 2007). Having found that Vps15 and Vps34 are required for efficient transcription elongation through various CDS driven by the *GAL1* promoter, we next asked whether these proteins are also required for targeting of active *GAL1* to the nuclear periphery. An array of Lac repressor binding sites was integrated downstream of the *GAL1* gene in wild type, *vps15*Δ and *vps34*Δ strains expressing a GFP fusion to Lac repressor (Straight *et al.* 1996; Brickner *et al.* 2007). Cells were shifted to galactose medium for 2 hr and the fraction of cells in the population in which *GAL1* colocalized with the nuclear periphery (marked with the nuclear pore protein Nsp1; Figure 6A) was scored (Brickner *et al.* 2010). A random distribution results in ~25–30% colocalization (Brickner and Walter 2004). In agreement with previous findings (Brickner *et al.* 2007), in the WT strain, *GAL1* localized at the nuclear periphery in 35 ± 2% of cells cultured in glucose and 65 ± 5% of cells grown with galactose. In the *vps15*Δ and *vps34*Δ mutant, we observed a strong defect in the targeting of *GAL1* to the nuclear periphery in galactose (32 ± 2% and 40 ± 4%, respectively) (Figure 6B). The *INO1* gene also is targeted to the nuclear periphery in WT cells cultured without inositol, which derepresses *INO1* transcription (Brickner and Walter 2004). Using a set of strains with Lac repressor binding sites integrated at *INO1*, we found that both *vps15*Δ and *vps34*Δ evoke marked reductions in *INO1* localization under derepressing conditions (Figure 6C). Thus,

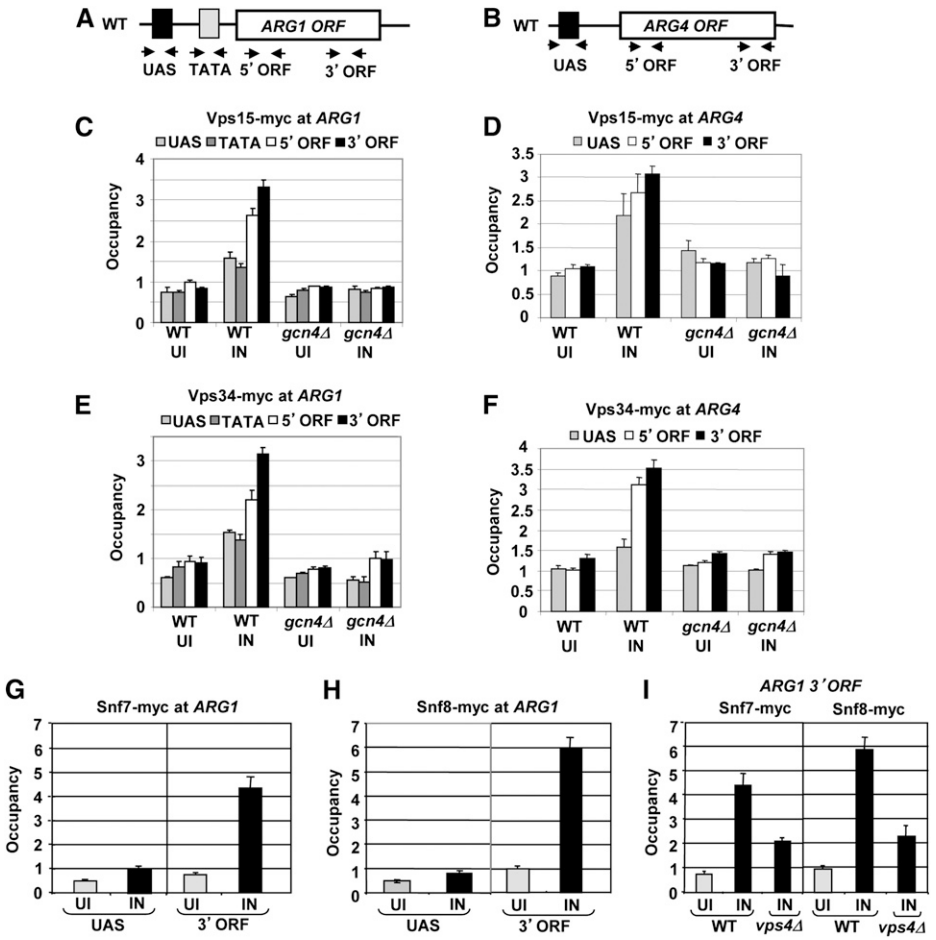

Figure 7 Transcription-dependent recruitment of Vps factors at Gcn4 target genes *ARG1* and *ARG4*. (A–D) ChIP analysis of myc-tagged Vps15 in *VPS15-myc*$_{13}$ strains NGY26 (WT) and NGY28 (*gcn4Δ*) at *ARG1* (A and C) and *ARG4* (B and D), using the primers depicted schematically in A and B, respectively, and control primer ChrV-1 listed in Table 4. (E and F) ChIP analysis of Vps34-myc in *VPS34-myc*$_{13}$ strains NGY27 (WT) and NGY29 (*gcn4Δ*) at *ARG1* (E) and *ARG4* (F) using the primers depicted in A and B and control primer ChrV-1 listed in Table 4. (G–I) ChIP analysis of Snf7-myc (G and I) at *ARG1* in *SNF7-myc*$_{13}$ strain FZY610 and *vps4Δ SNF7-myc*$_{13}$ strain FZY642, and of Snf8-myc in *SNF8-myc*$_{13}$ strain FZY644 and *vps4Δ SNF8-myc*$_{13}$ strain FZY657 (listed in Table 1) using the primers depicted in A and the control primers *POL1CDS* listed in Table 4. For all experiments, cells were cultured in SC −Ilv and either treated with 0.5 μM sulfometuron methyl (SM) for 30 min to induce Gcn4 (IN) or left untreated (UI). Cross-linked chromatin was immunoprecipitated with anti-myc antibodies and analyzed as in Figure 3A. Immunoprecipitations were conducted in duplicate on at least two chromatin samples prepared from two replicate cultures and the PCR analysis of precipitated DNA sequences was conducted in duplicate for each immunoprecipitated sample. Error bars represent the standard error of the mean (SEM).

Vps15 and Vps34 are required for normal targeting of the activated *GAL1* and *INO1* genes to the nuclear periphery.

Vps15 and Vps34 are cotranscriptionally cross-linked to the CDS of various yeast genes

Having found that *vps15Δ* and *vps34Δ* mutations reduce the efficiency of transcription elongation, cotranscriptional recruitment of NuA4, and targeting of several activated genes to the nuclear periphery, we wondered whether Vps15, Vps34, and other Vps factors could be physically associated with sites of transcription in yeast cells. This possibility was stimulated by reports (discussed below) that Vps factors from other species can be found in the nucleus in association with chromatin, or copurified with transcription elongation factors. To test this possibility in yeast, we first conducted ChIP analysis of functional myc-tagged versions of Vps15, Vps34, Snf7, and Snf8 at the Gcn4 target genes *ARG1* and *ARG4* in response to induction of Gcn4 by treatment with sulfometuron (SM), which inhibits biosynthesis of isoleucine and valine (Ilv). Our previous work has shown that Ilv starvation with SM evokes a rapid increase in Gcn4 occupancy of UAS elements, followed by recruitment of coactivators Mediator and SwItch/Sucrose NonFermentable (SWI/SNF) to the UAS and the HAT complexes Spt-Ada-Gcn5-acetyltransferase complex (SAGA) and NuA4 to both the UAS and CDS of various Gcn4 target genes (Govind *et al.* 2005; Qiu *et al.* 2005; Govind *et al.* 2007; Ginsburg *et al.* 2009).

Interestingly, we found that Vps15, Vps34, Snf7, and Snf8 can all be detected in association with both *ARG1* and *ARG4* on transcriptional induction by Gcn4, and the occupancies of all four Vps factors is consistently higher in the 3′ end of the CDS *vs.* the UAS or promoter (TATA) regions (Figure 7, A–H, *cf.* IN *vs.* UN for WT strains). In the case of Vps15 and Vps34, we established that their increased occupancies at *ARG1* and *ARG4* on treatment with SM were completely dependent on Gcn4, being abrogated in isogenic *gcn4Δ* strains (Figure 7, C–F, *cf.* WT IN *vs. gcn4*Δ IN). We observed that Snf7, Vps15, and Vps34 are also associated with the *GAL1* gene, strictly during its induction by Gal4 in galactose medium, and again exhibiting higher occupancies in the CDS *vs.* UAS or promoter regions (Figure 8, A–D, *cf.* Gal *vs.* Raf). Furthermore, Vps15 and Vps34 were detected in association with the *ADH1* and *PMA1* CDS, two genes transcribed constitutively in amino acid and glucose-containing medium (Figure 8, E–G).

The fact that occupancies of Vps factors are consistently higher in CDS *vs.* UAS or promoter, suggests that their recruitment requires elongating Pol II and not merely activator binding at the UAS. Supporting this idea, deleting the TATA element at *ARG1*, which reduces Pol II in the CDS, likewise reduces Vps15 and Vps34 occupancies at *ARG1* (Figure 9,

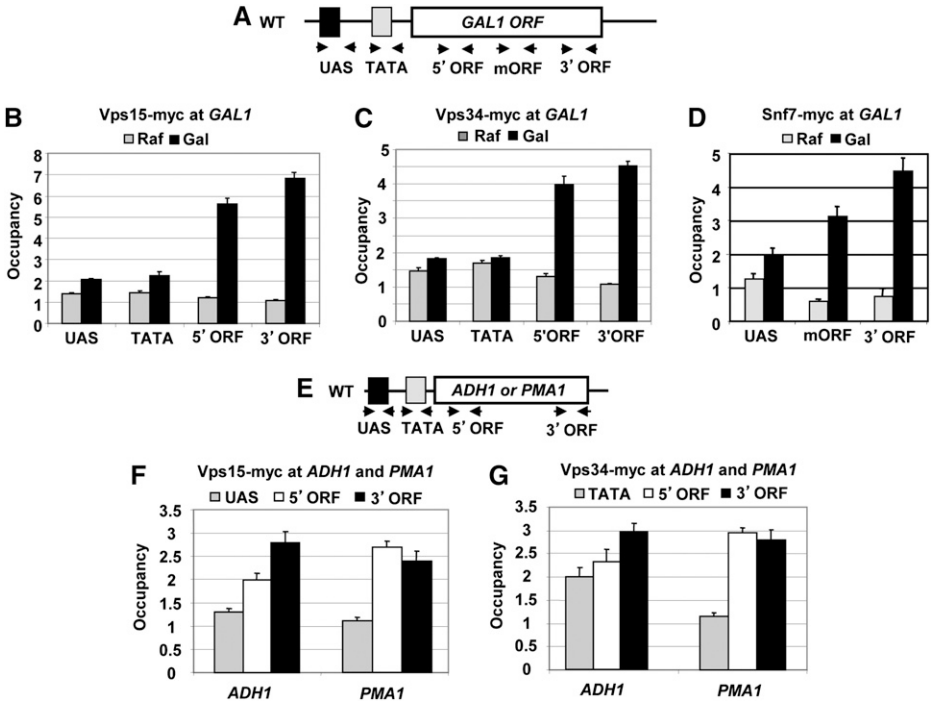

Figure 8 Recruitment of Vps factors to the CDS at *GAL1*, *ADH1*, and *PMA1*. (A–D) ChIP analysis of Vps15-myc in *VPS15-myc$_{13}$* strain NGY26 (B), Vps34-myc in *VPS34-myc$_{13}$* strain NGY27 (C), and Snf7-myc in *SNF7-myc$_{13}$* strain FZY610 (D) conducted for *GAL1* using the primers depicted in A and control primer ChrV-1 for B and C, *POL1 CDS* for C listed in Table 4. Cells were cultured and ChIP analysis was conducted as described in Figure 3A. (F and G) ChIP analysis of Vps15-myc in NGY26 and Vps34-myc in NGY27 conducted for *ADH1* and *PMA1* using the primers depicted in E and ChrV-1 as control listed in Table 4. Cells were grown to mid-log phase in SC −Ilv and induced with 0.5 μm of SM for 30 min. ChIP analysis was performed as in Figure 3A. Immunoprecipitations were conducted in duplicate on at least two chromatin samples prepared from two replicate cultures and the PCR analysis of precipitated DNA sequences was conducted in duplicate for each immunoprecipitated sample. Error bars represent the standard error of the mean (SEM).

A–D, *cf*. WT *vs*. *TATA*Δ). We showed previously that this *arg1-TATAΔ* mutation does not reduce the UAS occupancy of Gcn4 itself (Qiu *et al.* 2006).

The recruitment of histone-modifying enzymes, elongation and termination factors, and mRNA processing factors that function during transcription elongation is stimulated by the heptad repeats ($Tyr_1Ser_2Pro_3Thr_4Ser_5Pro_6Ser_7$) in the C-terminal domain of Pol II subunit Rpb1 (Pol II CTD), dependent on phosphorylation of the CTD repeats on Ser_2, Ser_5, or Ser_7 by various cyclin-dependent kinases (Phatnani and Greenleaf 2006; Buratowski 2009). Cdk7 (Kin28 in yeast) is the enzyme responsible for the majority of Ser_5 and Ser_7 CTD phosphorylation in yeast cells (Tietjen *et al.* 2010; Bataille *et al.* 2012). As expected, we observed that the occupancy of Rpb1 harboring Ser_5-phosphorylated CTD repeats (S5P) is higher at the promoter and 5′ end *vs.* the 3′ end of the CDS at *ARG1*, and inhibiting an analog-sensitive (as) version of Kin28 with an ATP analog reduced the occupancy of the S5P form of Rpb1 (Figure 9E), while having little effect on levels of total Pol II (Rpb3) at *ARG1* (Figure 9F). Interestingly, the occupancy of Vps34 was reduced at the 3′ end of *ARG1* on inhibition of Kin28-as (Figure 9G), leading to a reduced Vps34:Rpb3 ratio at this location (Figure 9H). Similar results were obtained for Vps15 on inhibition of kin28-as (Figure 9, I–K). This finding suggests that S5P or S7P enhances, directly or indirectly, the cotranscriptional association of these Vps factors at promoter-distal locations. We conclude that association of the Vps15 and Vps34 with CDS is coupled to transcription elongation and stimulated by CTD phosphorylation by Kin28.

Interestingly, we found that *vps4Δ* cells display reduced association of ESCRT-II factor Snf8 and ESCRT-III component Snf7 with the *ARG1* CDS (Figure 7I). It is known that cells lacking the AAA-ATPase Vps4 fail to produce ILVs and to recycle ESCRT factors to the cytoplasm, causing accumulation of ESCRT-III component Snf7 at the MVB (Babst *et al.* 1998). The fact that association of Snf7 and Snf8 with the *ARG1* CDS is diminished in *vps4Δ* cells is consistent with the idea that these ESCRT factors are partitioned between endosome- and nucleus-associated pools and that their impaired recycling from the MVB to the cytoplasm in *vps4Δ* cells decreases their association with chromatin.

We went on to examine association of Myc-tagged versions of several other Vps factors with *ARG1* or *GAL1* CDS and observed induction-dependent association of Vps4, Vps27, and Vps10 at *ARG1* and Vps45, Vps10 and Pep7 at *GAL1* at levels comparable to those described above for Vps15, Vps34, Snf7, and Snf8 (Figure 10, A–D). In parallel, we analyzed two different functional myc-tagged protein synthesis initiation factors, eIF4E/Cdc33 and eIF3a/Tif32, that we expected to be primarily, if not exclusively cytoplasmic. We observed twofold or less increases in association of Cdc33-myc and Tif32-myc occupancy on transcriptional induction at *ARG1* (Figure 10C), and also at *ARG4* and *GAL1* (data not shown). Thus, although induction-dependent chromatin association of the translation initiation factors is not negligible, it is significantly lower in magnitude than that seen for the Vps factors.

Fractions of Vps15 and Vps34 colocalize with nucleoporin Nsp1 at edges of nucleus–vacuole junctions

To examine further the possibility that fractions of Vps15 and Vps34 are physically associated with transcribed genes in the nucleus, we visualized GFP fusions to these proteins in

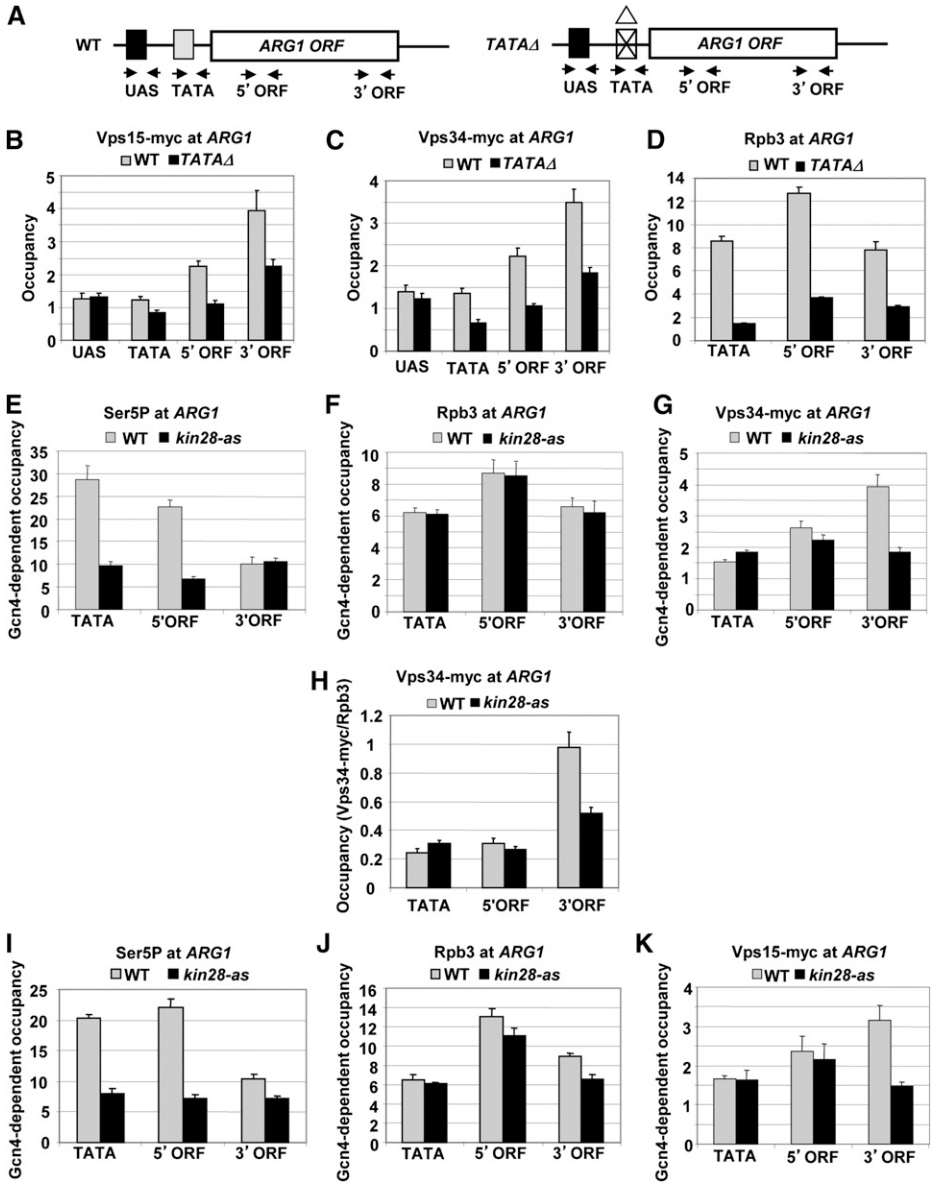

Figure 9 Cotranscriptional recruitment of Vps15-myc and Vps34-myc is stimulated by the Pol II CTD kinase Cdk7/Kin28. (A–D) ChIP analysis at *ARG1* conducted for Vps15-myc in WT (NGY26) and *arg1-TATAΔ* (NGY56) strains harboring *VPS15-myc*$_{13}$ (B), and for Vps34-myc in WT (NGY27) and *arg1-TATAΔ* (NGY57) strains harboring *VPS34-myc13* (C), and for Rpb3 in WT (NGY27) and *arg1-TATAΔ* (NGY57) strains (D), using primers depicted in A and B and control primer ChrV-1 listed in Table 4. Cells were grown to mid-log phase in SC −Ilv and induced with 0.5 μm of SM for 30 min. Occupancies of Vps34-myc (C) and Rbp3 (D) were measured in the same chromatin extracts. (E–H) ChIP analysis of Rpb1 phosphorylated on Ser$_5$ of its CTD (Ser5P, E), Rpb3 (F) and Vps34-myc (G and H) was conducted on the same chromatin extracts from *KIN28 VPS34-myc*$_{13}$ strain NGY69 (WT), *kin28-as VPS34-myc*$_{13}$ strain NGY71 (*kin28-as*), and *gcn4Δ VPS34-myc*$_{13}$ strain NGY29. Cells were grown in SC −Ilv and treated with 1-NA-PP1 [1- (1, 1-dimethylethyl)- 3- (1- naphthalenyl)- 1H-pyrazolo[3, 4- d]pyrimidin- 4- amine] at 12 μM for 42 min and SM 0.5 μm for the last 30 min of the NAPP1 treatment. ChIP analysis was conducted as in Figure 3A and values obtained for the *KIN28* and *kin28-as* strains were normalized to those obtained for the *gcn4Δ* strain to produce the plotted Gcn4-dependent occupancies in E–G. H presents the ratios of occupancies in G and F. **(**I–K**)** ChIP analysis conducted as in E–G except using *KIN28VPS15-myc*$_{13}$ strain NGY68, *kin28-as VPS15-myc*$_{13}$ strain NGY70, and *gcn4Δ VPS15-myc*$_{13}$ strain NGY28. For all ChIP experiments, immunoprecipitations were conducted in duplicate on at least two chromatin samples prepared from two replicate cultures and the PCR analysis of precipitated DNA sequences was conducted in duplicate for each immunoprecipitated sample. Error bars represent the standard error of the mean (SEM).

living cells that also contain RFP or BFP fusions to the nucleoporin Nsp1 (Aitchison and Rout 2012) or an mCherry fusion to transcription elongation factor Spt4. Consistent with previous results (Huh *et al.* 2003; Obara *et al.* 2006), both Vps15-GFP and Vps34-GFP were found primarily in cytoplasmic punctae reflecting their association with endosomes and the outer membrane of the vacuole. Nsp1-RFP was found in punctae localized at the nuclear rim in the manner expected for a nucleoporin, as observed previously (MacKinnon *et al.* 2009). Under conditions where the Vps proteins were found cross-linked to transcribed chromatin, including 30 min cultivation in SC −galactose medium, we did not observe any obvious accumulation of Vps34 or Vps15 inside the nucleus. However, a fraction of the Vps-GFP punctae colocalized with Nsp1-RFP at the edges of junctions formed between the nucleus and vacuole, from which Nsp1 is largely excluded. This pattern was observed in essentially all cells we examined in cultures prepared in SC with glucose, raffinose, or galactose as carbon source (Supporting Information, Figure S1 and Figure S2). It is known that NV junctions are mediated by interactions between vacuolar membrane protein Vac8 and outer nuclear-membrane protein Nvj1 and are devoid of nuclear pores (Pan *et al.* 2000). Our time-lapse microscopic observations suggest that Vps34-GFP or Vps15-GFP punctae at the vacuolar membrane are dynamic and transiently associate with nuclear pores (Nsp1-RFP) at the edges of NV junctions (Movies M1–6 in File S1, File S2, File S3, File S4, File S5, and FileS6). Interestingly, when cells were cultivated overnight on rich glucose (YPD) agar medium and then investigated under agarose strips cast in minimal galactose

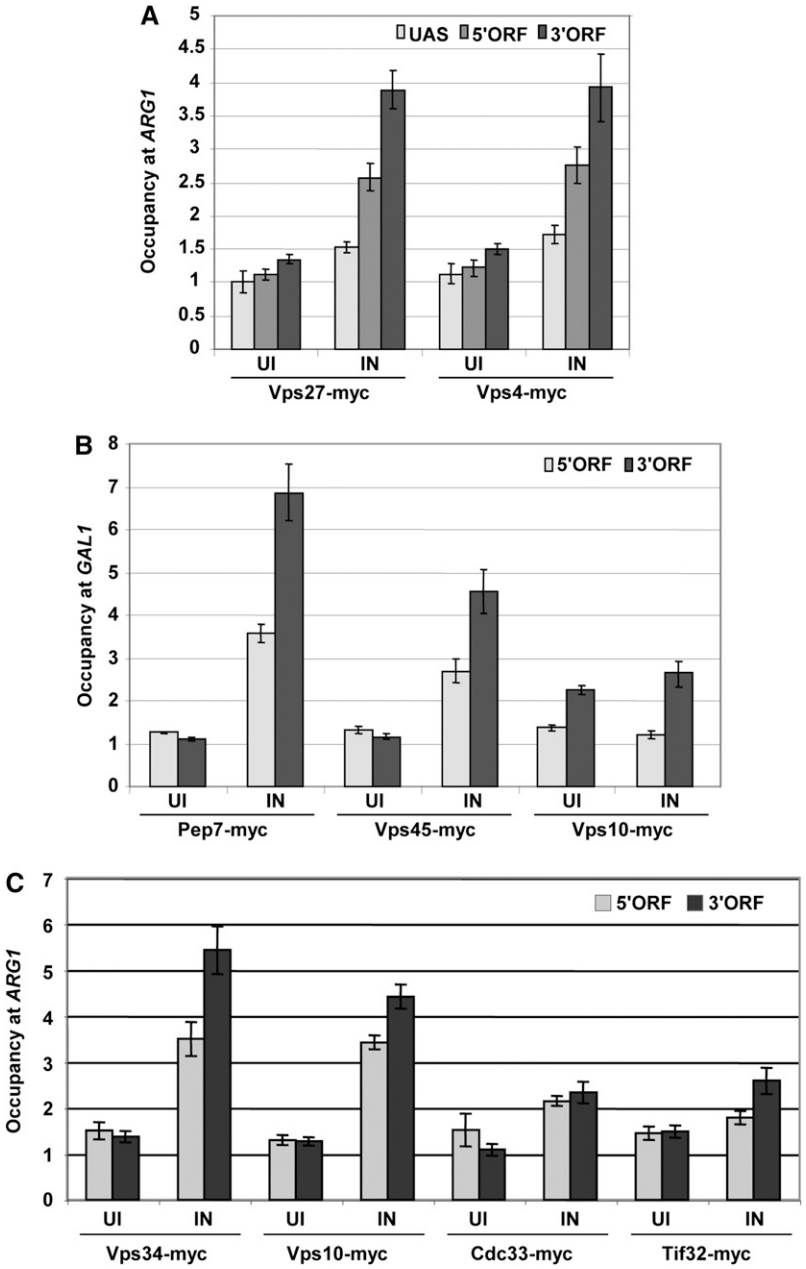

Figure 10 Vps factors exhibit higher occupancies of transcribed *ARG1* CDS than do translation factors eIF4E and eIF3a. (A and C) ChIP analysis of Vps27-myc and Vps4-myc in strains NGY98 and NGY99, respectively (A), and Vps34-myc, Vps10-myc, eIF4E/Cdc33-myc, and eIF3a/Tif32-myc in strains NGY27, NGY116, H3881, and H3879, respectively (C), all conducted for *ARG1* as described in Figure 7. Except control primer for Cdc-33my and Tif32-myc was POL1CDS (B) ChIP analysis of Pep7-myc, Vps45-myc, and Vps10-myc in NGY100, NGY101, and NGY116, respectively, conducted for *GAL1* as described in Figure 3A. Immunoprecipitations were conducted in duplicate on at least two chromatin samples prepared from two replicate cultures and the PCR analysis of precipitated DNA sequences was conducted in duplicate for each immunoprecipitated sample. Error bars represent the standard error of the mean (SEM).

medium, >50% of them displayed obvious overlapping signals of Vps34-GFP or Vps15-GFP with Nsp1-RFP (Figure S3).

Spt4-mCherry, examined as a nuclear marker, showed relatively homogenous nuclear localization in the manner expected for a transcription elongation factor distributed throughout the nucleoplasm in exponentially growing cells (Huh *et al.* 2003). We found that in the cells shifted from YPD plates to minimal galactose medium before microscopy, Spt4-mCherry usually did not occupy the entire nuclear space defined by the Nsp1-BFP nuclear rim. In rare instances a portion of Vps15 appeared to be located inside the nucleus of these cells (Figure S4A), and analysis of optical sections revealed that the Vps15-GFP signal was surrounded by Spt4-mCherry material within the nuclear rim defined by Nsp1-BFP (see layer 2). Similarly, as shown in Figure S4B, the Vps15-GFP signal could be observed as an inclusion inside the Spt4-mCherry domain (layer 2). Together, our microscopic findings indicate that a fraction of Vps15 and Vps34 are in proximity to nuclear pores at the edges of NV junctions, and that rarely, the Vps15-GFP fusion protein can be found within the nucleus under certain culture conditions.

Discussion

We demonstrated previously that eliminating certain *VPS* genes whose products are involved in Golgi-to-vacuole vesicular protein trafficking reduced the ability of transcriptional activator Gcn4 to stimulate PIC assembly and transcription initiation *in vivo*. Based on the results of assaying a *GAL1-lacZ*

reporter gene, it appeared that the function of Gal4 was also impaired by the *vps15Δ* and *vps34Δ* mutations, which reduced *GAL1-lacZ* expression by 60 and 80%, respectively (Zhang *et al.* 2008). We showed here, however, that Gal4 function in PIC assembly appears to be normal in *vps15Δ* and *vps34Δ* cells and presented several lines of evidence that the reductions in Gal4-dependent *lacZ* reporter expression observed in these mutants is engendered by a defect at the elongation stage of transcription. Indeed, Aguilera and colleagues have established that reduced mRNA production from *lacZ* reporters and certain native genes with long or GC-rich CDS are hallmarks of mutations in various elongation factors in yeast (Chavez *et al.* 2001; Rondon *et al.* 2003a, 2004; Morillo-Huesca *et al.* 2006; Tous *et al.* 2011). We consistently observed decreased mRNA expression from several such reporters, all driven by the *GAL1* promoter, in *vps15Δ* and *vps34Δ* cells. Employing a ChIP analysis of the kinetics of Pol II elongation *in vivo* (Mason and Struhl 2005), modified to include *lacZ* CDS, we also obtained evidence that elimination of Vps15 or Vps34 reduces the rate of Pol II elongation through *lacZ* CDS *in vivo*.

We further identified defects in cotranscriptional recruitment of the HAT complex NuA4 to the *GAL1* CDS in *vps15Δ* and *vps34Δ* cells. Considering that conditional inactivation of the HAT subunit of NuA4 (Esa1) also impairs the rate of Pol II elongation *in vivo* (Ginsburg *et al.* 2009), the reduced NuA4 occupancy in CDS we observed in *vps15Δ* and *vps34Δ* mutants could contribute to their transcription elongation defects. We additionally demonstrated that *vps15Δ* and *vps34Δ* cells are defective for localization of activated *GAL1* and *INO1* to the nuclear periphery (gene positioning), a process that requires a number of nuclear pore complex (NPC) proteins or associated factors and likely facilitates coordination of transcription and mRNP biogenesis with mRNA export at nuclear pores (Egecioglu and Brickner 2011). Indeed, the nucleoporin Nup2 is required for targeting of both *GAL1* and *INO1* to the nuclear periphery (Brickner *et al.* 2007), and the TREX-2/THSC (nuclear pore-associated complex composed of Sac3–Thp1–Cdc31) complex is located at nuclear pores and is required for gene positioning of *GAL1* (Cabal *et al.* 2006) and efficient mRNA export (Fischer *et al.* 2002; Lei *et al.* 2003).

Our ability to demonstrate an elongation defect for particular genes with long or GC-rich CDS, such as *lacZ*, does not rule out a general requirement for Vps factors for efficient elongation, as transcription of most genes in yeast is unaffected in mutants lacking only a single elongation factor. The elongation process appears to be overdetermined (Mason and Struhl 2005), such that only a few specialized genes require a full complement of cofactors for efficient transcription elongation *in vivo* (Chavez *et al.* 2001). Whereas the elongation defect described here likely applies broadly to many genes, the impairment of transcription initiation we observed previously in *vps* mutants (Zhang *et al.* 2008) is restricted to a subset of activators that includes Gcn4, but not Gal4, and seems to involve a signaling pathway that responds to sterol limitation (Mousley *et al.* 2012). Hence, we now interpret the dramatic reductions in expression of Gcn4-dependent *lacZ* reporters we observed previously in *vps15Δ* and *vps34Δ* mutants (Zhang *et al.* 2008) to be the compound effect of reduced PIC assembly by Gcn4 and impaired transcription elongation through *lacZ* CDS.

Given their well-established functions in vesicular protein trafficking, we anticipated that Vps15 and Vps34 would promote transcription elongation by an indirect mechanism. Hence, we were surprised to obtain evidence by ChIP assays for physical association of these and several other functionally related Vps proteins with transcribed chromatin. The Vps factors consistently displayed higher occupancies of the CDS *vs.* UAS or promoter regions of the examined genes, consistent with a widespread role in transcription elongation. The CDS occupancies of the Vps proteins were lower than we observed previously for canonical elongation factors, including Spt4, Spt5, Bur2, and the Paf1C complex (Qiu *et al.* 2006, 2009), but they were comparable to the occupancies of subunits of SAGA (Govind *et al.* 2007), NuA4 (Ginsburg *et al.* 2009), and histone deacetylase complexes (Govind *et al.* 2010), and they were significantly higher than the twofold or less enrichment of two different protein synthesis factors we analyzed at Gcn4 and Gal4 target genes. Importantly, as observed for conventional elongation factors, the association of Vps proteins with *ARG1* or *GAL1* CDS was strongly dependent on target gene transcription, occurring at high levels only under conditions where the relevant transcriptional activators are induced (Gcn4) or functional (Gal4). In addition, the TATA promoter element is required for high-level Vps15 and Vps34 occupancies at *ARG1* under inducing conditions, and Vps15 and Vps34 occupancies of *ARG1* CDS were stimulated by the Pol II CTD kinase Cdk7/Kin28—a characteristic of numerous factors involved in cotranscriptional histone modifications, mRNA processing or nuclear export, and the elongation or termination phases of transcription (Phatnani and Greenleaf 2006; Govind *et al.* 2007; Pascual-Garcia *et al.* 2008; Ginsburg *et al.* 2009; Govind *et al.* 2010; Qiu *et al.* 2012).

The specific association of Vps factors with transcribed coding sequences raises the possibility that they function in association with the chromatin to promote transcription elongation rather than influencing the process indirectly at the endosome. In this view, certain Vps factors would be partitioned between cytoplasm and nucleus and have dual functions in protein trafficking and transcription in these two compartments. Further evidence for this partitioning is provided by our finding that association of Snf7/Vps32 and Snf8/Vps22 with *ARG1* chromatin is diminished in *vps4*Δ cells, in which Snf7 accumulates on the MVB outer membrane owing to a defect in ILV formation and recycling of ESCRT-III factors back to the cytoplasm (Babst *et al.* 1998). By fluorescence microscopy of living cells, we also observed association of a fraction of Vps15-GFP and Vps34-GFP fusions with an RFP fusion to nucleoporin Nsp1 at the edges of NV junctions. This pattern of vacuole/nucleus interaction

was observed frequently under various growth conditions. Our time-lapse microscopy revealed that association of Vps punctae with the edges of NV junctions is highly dynamic, such that Vps15/Vps34 colocalization with nuclear pores is transient and observed only in particular optical layers. These findings raise the possibility of a dynamic interaction of Vps15/Vps34 proteins with actively transcribed genes at nuclear pores, which could be consistent with their requirement for efficient gene localization to the nuclear periphery. It is unclear, however, whether an association of Vps15/Vps34 with nuclear pores that is restricted to the borders of NV junctions could account for their widespread cross-linking to transcribed genes and their apparently general effect on transcription elongation. It is worth noting that the Vps34 homolog in *Caenorhabditis elegans* is concentrated in a perinuclear location, although this cellular location has been connected so far only with its role in vesicle budding from the outer nuclear membrane directed toward the cell periphery (Roggo *et al.* 2002).

Despite our evidence for physical association of a fraction of Vps15 and Vps34 with transcribed chromatin and nuclear pores, we have been unable to observe a defect in Pol II elongation in whole cell extracts of *vps34Δ* cells using a DNA template containing two G-less cassettes flanking *lacZ* CDS (data not shown). This assay was employed previously to provide evidence for direct roles of various factors in transcription elongation, including Spt4 and subunits of the THO complex (Rondon *et al.* 2003a,b and 2004). Accordingly, the elongation defect we observed in *vps15Δ* and *vps34Δ* cells presumably involves an aspect of nuclear structure or nucleus–cytoplasm interaction that cannot be recapitulated in homogenized cell extracts. However, we cannot eliminate the possibility that the elongation defect we documented in *vps15Δ* and *vps34Δ* mutants represents an indirect consequence of a defect in vesicular protein trafficking in the cytoplasm that is incidental to the association of Vps15 and Vps34 with transcribed chromatin and nuclear pores.

Notwithstanding this last reservation, one interesting hypothesis would be that Vps15/Vps34 function at the nuclear periphery to promote transcription elongation of activated genes localized to nuclear pores. Vps34 generates PI(3)P at endosomal membranes, which recruits ESCRT-0 factor Vps27 via its FYVE (Fab1, YGL023, Vps27, and EEA1) domain (Raiborg and Stenmark 2009). To our knowledge, there is no prior evidence that Vps27 or any other known yeast FYVE protein (Pep7, Fab1, Pib1, and Pib2) functions in the nucleus. (Although the FYVE factor Fab1 regulates assembly of the Cti6/Cyc8/Tup1 transcriptional cofactor complex, it performs this function at endosomes (Han and Emr 2011). Interestingly, however, plant homeodomain (PHD) fingers can bind various phosphoinositide phosphates (PIPs), including PI(3)P (Gozani *et al.* 2003), and are found in many chromatin and transcription-related proteins, including the Yng2 subunit of NuA4 (http://smart.embl.de/). Given our finding that transcription-coupled recruitment of NuA4 to the *GAL1* CDS is diminished in *vps15Δ* and *vps34Δ* cells, it could be proposed that PI(3)P produced by Vps15/Vps34 on the nuclear membrane, possibly at nuclear pores, stimulates recruitment of NuA4 and other PHD-containing transcription cofactors to enhance elongation by Pol II. A precedent for such a mechanism is provided by evidence indicating that mammalian Ing2, an histone deacetylase complex (HDAC) component, is recruited to chromatin by a nuclear pool of PI(5)P via its PHD finger, where it regulates p53 acetylation and apoptosis in response to DNA damage (Gozani *et al.* 2003). Indeed, there is increasing evidence for phosphoinositides in the inner nuclear periphery and for isoforms of phosphoinositide kinases being located inside the nucleus (Barlow *et al.* 2010).

If PI(3)P is produced by Vps15/Vps34 on the nuclear membrane in the manner just proposed, this might account for our ability to detect transcription-dependent chromatin association of the FYVE-containing proteins Vps27 and Pep7 by ChIP assays. Moreover, the similar ChIP results observed for Vps factors Snf7, Snf8, Vps4, Vps45, and possibly Vps10, might reflect their association, direct or indirect, with Vps27 or Pep7. However, it seems more difficult to account for our evidence that these other Vps proteins also contribute to efficient transcription elongation, albeit to a lesser extent than do Vps15 and Vps34. One possibility is that impairing vesicular protein trafficking in the cytoplasm by deletions of various Vps factors reduces the nucleus-associated pools of Vps15 and Vps34 and thereby impairs transcription elongation indirectly.

There are other indications of nuclear functions for certain Vps proteins, including the fact that mammalian ESCRT-II was first purified in association with Pol II elongation factor Eleven-Nineteen Lysine-rich Leukemia (ELL) (Shilatifard 1998), and a report that plant Vps34 colocalizes with sites of transcription in plant cell nuclei (Bunney *et al.* 2000). In addition, the mammalian homolog of the ESCRT-III-related protein Vps46/Did2, when overexpressed, was found to enter the nucleus and locally condense chromatin and to produce a gene-silencing phenotype in *Xenopus* embryos (Stauffer *et al.* 2001). Clearly more work is required to determine at the molecular level exactly how Vps factors promote transcription elongation in yeast cells and whether the mechanisms involved depend on their physical interaction with chromatin and nuclear pores.

Acknowledgments

We thank Sebastián Chávez, Andrés Aguilera, Henrik Dohlman, Steven Hahn, Kristine Willis, Roger Tsien, and the Yeast Resource Center at the University of Washington for gifts of plasmids, and Thomas Dever for useful suggestions. This work was supported in part by the Intramural Research Program of the National Institutes of Health. J.H. was supported by P305/12/0480 and RVO61388971, and D.G.B. and J.H.B. were supported by a W. M. Keck Young Scholars in Medical Research Award.

Literature Cited

Aitchison, J. D., and M. P. Rout, 2012 The yeast nuclear pore complex and transport through it. Genetics 190: 855–883.

Alani, E., L. Cao, and N. Kleckner, 1987 A method for gene disruption that allows repeated use of *URA3* selection in the construction of multiply disrupted yeast strains. Genetics 116: 541–545.

Babst, M., B. Wendland, E. J. Estepa, and S. D. Emr, 1998 The Vps4p AAA ATPase regulates membrane association of a Vps protein complex required for normal endosome function. EMBO J. 17: 2982–2993.

Barlow, C. A., R. S. Laishram, and R. A. Anderson, 2010 Nuclear phosphoinositides: a signaling enigma wrapped in a compartmental conundrum. Trends Cell Biol. 20: 25–35.

Bataille, A. R., C. Jeronimo, P. E. Jacques, L. Laramee, M. E. Fortin *et al.*, 2012 A universal RNA polymerase II CTD cycle is orchestrated by complex interplays between kinase, phosphatase, and isomerase enzymes along genes. Mol. Cell 45: 158–170.

Bowers, K., and T. H. Stevens, 2005 Protein transport from the late Golgi to the vacuole in the yeast Saccharomyces cerevisiae. Biochim. Biophys. Acta 1744: 438–454.

Boysen, J. H., and A. P. Mitchell, 2006 Control of Bro1-domain protein Rim20 localization by external pH, ESCRT machinery, and the Saccharomyces cerevisiae Rim101 pathway. Mol. Biol. Cell 17: 1344–1353.

Brickner, D. G., I. Cajigas, Y. Fondufe-Mittendorf, S. Ahmed, P. C. Lee *et al.*, 2007 H2A.Z-mediated localization of genes at the nuclear periphery confers epigenetic memory of previous transcriptional state. PLoS Biol. 5: e81.

Brickner, D. G., W. Light, and J. H. Brickner, 2010 Quantitative localization of chromosomal loci by immunofluorescence. Methods Enzymol. 470: 569–580.

Brickner, J. H., and P. Walter, 2004 Gene recruitment of the activated INO1 locus to the nuclear membrane. PLoS Biol. 2: e342.

Bryant, G. O., and M. Ptashne, 2003 Independent recruitment in vivo by Gal4 of two complexes required for transcription. Mol. Cell 11: 1301–1319.

Bunney, T. D., P. A. Watkins, A. F. Beven, P. J. Shaw, L. E. Hernandez *et al.*, 2000 Association of phosphatidylinositol 3-kinase with nuclear transcription sites in higher plants. Plant Cell 12: 1679–1688.

Buratowski, S., 2009 Progression through the RNA polymerase II CTD cycle. Mol. Cell 36: 541–546.

Cabal, G. G., A. Genovesio, S. Rodriguez-Navarro, C. Zimmer, O. Gadal *et al.*, 2006 SAGA interacting factors confine sub-diffusion of transcribed genes to the nuclear envelope. Nature 441: 770–773.

Casolari, J. M., C. R. Brown, S. Komili, J. West, H. Hieronymus *et al.*, 2004 Genome-wide localization of the nuclear transport machinery couples transcriptional status and nuclear organization. Cell 117: 427–439.

Chavez, S., T. Beilharz, A. G. Rondon, H. Erdjument-Bromage, P. Tempst *et al.*, 2000 A protein complex containing Tho2, Hpr1, Mft1 and a novel protein, Thp2, connects transcription elongation with mitotic recombination in *Saccharomyces cerevisiae*. EMBO J. 19: 5824–5834.

Chavez, S., M. Garcia-Rubio, F. Prado, and A. Aguilera, 2001 Hpr1 is preferentially required for transcription of either long or G+C-rich DNA sequences in Saccharomyces cerevisiae. Mol. Cell. Biol. 21: 7054–7064.

Egecioglu, D., and J. H. Brickner, 2011 Gene positioning and expression. Curr. Opin. Cell Biol. **23:** 338–354.

Exinger, F., and F. Lacroute, 1992 6-Azauracil inhibition of GTP biosynthesis in Saccharomyces cerevisiae. Curr. Genet. 22: 9–11.

Fischer, T., K. Strasser, A. Racz, S. Rodriguez-Navarro, M. Oppizzi *et al.*, 2002 The mRNA export machinery requires the novel Sac3p-Thp1p complex to dock at the nucleoplasmic entrance of the nuclear pores. EMBO J. 21: 5843–5852.

Giaever, G., A. M. Chu, L. Ni, C. Connelly, L. Riles *et al.*, 2002 Functional profiling of the Saccharomyces cerevisiae genome. Nature 418: 387–391.

Gietz, R. D., and A. Sugino, 1988 New yeast-Escherichia coli shuttle vectors constructed with in vitro mutagenized yeast genes lacking six-base pair restriction sites. Gene 74: 527–534.

Ginsburg, D. S., C. K. Govind, and A. G. Hinnebusch, 2009 The NuA4 lysine acetyltransferase Esa1 is targeted to coding regions and stimulates transcription elongation with Gcn5. Mol. Cell. Biol. 29: 6473–6487.

Govind, C. K., S. Yoon, H. Qiu, S. Govind, and A. G. Hinnebusch, 2005 Simultaneous recruitment of coactivators by Gcn4p stimulates multiple steps of transcription in vivo. Mol. Cell. Biol. 25: 5626–5638.

Govind, C. K., F. Zhang, H. Qiu, K. Hofmeyer, and A. G. Hinnebusch, 2007 Gcn5 promotes acetylation, eviction, and methylation of nucleosomes in transcribed coding regions. Mol. Cell 25: 31–42.

Govind, C. K., H. Qiu, D. S. Ginsburg, C. Ruan, K. Hofmeyer *et al.*, 2010 Phosphorylated Pol II CTD recruits multiple HDACs, including Rpd3C(S), for methylation-dependent deacetylation of ORF nucleosomes. Mol. Cell 39: 234–246.

Gozani, O., P. Karuman, D. R. Jones, D. Ivanov, J. Cha *et al.*, 2003 The PHD finger of the chromatin-associated protein ING2 functions as a nuclear phosphoinositide receptor. Cell 114: 99–111.

Han, B. K., and S. D. Emr, 2011 Phosphoinositide [PI(3,5)P2] lipid-dependent regulation of the general transcriptional regulator Tup1. Genes Dev. 25: 984–995.

Hartzog, G. A., T. Wada, H. Handa, and F. Winston, 1998 Evidence that Spt4, Spt5, and Spt6 control transcription elongation by RNA polymerase II in Saccharomyces cerevisiae. Genes Dev. 12: 357–369.

Hinnebusch, A. G., 2005 Translational regulation of GCN4 and the general amino acid control of yeast. Annu. Rev. Microbiol. 59: 407–450.

Huh, W. K., J. V. Falvo, L. C. Gerke, A. S. Carroll, R. W. Howson *et al.*, 2003 Global analysis of protein localization in budding yeast. Nature 425: 686–691.

Hurley, J. H., and S. D. Emr, 2006 The ESCRT complexes: structure and mechanism of a membrane-trafficking network. Annu. Rev. Biophys. Biomol. Struct. 35: 277–298.

Janke, C., M. M. Magiera, N. Rathfelder, C. Taxis, S. Reber *et al.*, 2004 A versatile toolbox for PCR-based tagging of yeast genes: new fluorescent proteins, more markers and promoter substitution cassettes. Yeast 21: 947–962.

Jenks, M. H., and D. Reines, 2005 Dissection of the molecular basis of mycophenolate resistance in Saccharomyces cerevisiae. Yeast 22: 1181–1190.

Jimeno, S., A. G. Rondon, R. Luna, and A. Aguilera, 2002 The yeast THO complex and mRNA export factors link RNA metabolism with transcription and genome instability. EMBO J. 21: 3526–3535.

Kamura, T., D. Burian, H. Khalili, S. L. Schmidt, S. Sato *et al.*, 2001 Cloning and characterization of ELL-associated proteins EAP45 and EAP20. a role for yeast EAP-like proteins in regulation of gene expression by glucose. J. Biol. Chem. 276: 16528–16533.

Lei, E. P., C. A. Stern, B. Fahrenkrog, H. Krebber, T. I. Moy *et al.*, 2003 Sac3 is an mRNA export factor that localizes to cytoplasmic fibrils of nuclear pore complex. Mol. Biol. Cell 14: 836–847.

Lin, Y. Y., Y. Qi, J. Y. Lu, X. Pan, D. S. Yuan *et al.*, 2008 A comprehensive synthetic genetic interaction network governing yeast histone acetylation and deacetylation. Genes Dev. 22: 2062–2074.

Liu, Y., C. Kung, J. Fishburn, A. Z. Ansari, K. M. Shokat *et al.*, 2004 Two cyclin-dependent kinases promote RNA polymerase II transcription and formation of the scaffold complex. Mol. Cell. Biol. 24: 1721–1735.

MacKinnon, M. A., A. J. Curwin, G. J. Gaspard, A. B. Suraci, J. P. Fernandez-Murray *et al.*, 2009 The Kap60-Kap95 karyopherin complex directly regulates phosphatidylcholine synthesis. J. Biol. Chem. 284: 7376–7384.

Mason, P. B., and K. Struhl, 2005 Distinction and relationship between elongation rate and processivity of RNA polymerase II in vivo. Mol. Cell 17: 831–840.

McPhillips, C. C., J. W. Hyle, and D. Reines, 2004 Detection of the mycophenolate-inhibited form of IMP dehydrogenase in vivo. Proc. Natl. Acad. Sci. USA 101: 12171–12176.

Morillo-Huesca, M., M. Vanti, and S. Chavez, 2006 A simple in vivo assay for measuring the efficiency of gene length-dependent processes in yeast mRNA biogenesis. FEBS J. 273: 756–769.

Mousley, C. J., P. Yuan, N. A. Gaur, K. D. Trettin, A. H. Nile *et al.*, 2012 A sterol-binding protein integrates endosomal lipid metabolism with TOR signaling and nitrogen sensing. Cell 148: 702–715.

Obara, K., T. Sekito, and Y. Ohsumi, 2006 Assortment of phosphatidylinositol 3-kinase complexes–Atg14p directs association of complex I to the pre-autophagosomal structure in Saccharomyces cerevisiae. Mol. Biol. Cell 17: 1527–1539.

Pan, X., P. Roberts, Y. Chen, E. Kvam, N. Shulga *et al.*, 2000 Nucleus-vacuole junctions in Saccharomyces cerevisiae are formed through the direct interaction of Vac8p with Nvj1p. Mol. Biol. Cell 11: 2445–2457.

Pascual-Garcia, P., C. K. Govind, E. Queralt, B. Cuenca-Bono, A. Llopis *et al.*, 2008 Sus1 is recruited to coding regions and functions during transcription elongation in association with SAGA and TREX2. Genes Dev. 22: 2811–2822.

Phatnani, H. P., and A. L. Greenleaf, 2006 Phosphorylation and functions of the RNA polymerase II CTD. Genes Dev. 20: 2922–2936.

Puria, R., S. A. Zurita-Martinez, and M. E. Cardenas, 2008 Nuclear translocation of Gln3 in response to nutrient signals requires Golgi-to-endosome trafficking in Saccharomyces cerevisiae. Proc. Natl. Acad. Sci. USA 105: 7194–7199.

Qiu, H., C. Hu, S. Yoon, K. Natarajan, M. J. Swanson *et al.*, 2004 An array of coactivators is required for optimal recruitment of TATA binding protein and RNA polymerase II by promoter-bound Gcn4p. Mol. Cell. Biol. 24: 4104–4117.

Qiu, H., C. Hu, F. Zhang, G. J. Hwang, M. J. Swanson *et al.*, 2005 Interdependent recruitment of SAGA and Srb mediator by transcriptional activator Gcn4p. Mol. Cell. Biol. 25: 3461–3474.

Qiu, H., C. Hu, C. M. Wong, and A. G. Hinnebusch, 2006 The Spt4p subunit of yeast DSIF stimulates association of the Paf1 complex with elongating RNA polymerase II. Mol. Cell. Biol. 26: 3135–3148.

Qiu, H., C. Hu, and A. G. Hinnebusch, 2009 Phosphorylation of the Pol II CTD by KIN28 enhances BUR1/BUR2 recruitment and Ser2 CTD phosphorylation near promoters. Mol. Cell 33: 752–762.

Qiu, H., C. Hu, N. A. Gaur, and A. G. Hinnebusch, 2012 Pol II CTD kinases Bur1 and Kin28 promote Spt5 CTR-independent recruitment of Paf1 complex. EMBO J. **31:** 3494–3505.

Raiborg, C., and H. Stenmark, 2009 The ESCRT machinery in endosomal sorting of ubiquitylated membrane proteins. Nature 458: 445–452.

Reid, G. A., and G. Schatz, 1982 Import of proteins into mitochondria. J. Biol. Chem. 257: 13062–13067.

Riles, L., R. J. Shaw, M. Johnston, and D. Reines, 2004 Large-scale screening of yeast mutants for sensitivity to the IMP dehydrogenase inhibitor 6-azauracil. Yeast 21: 241–248.

Roggo, L., V. Bernard, A. L. Kovacs, A. M. Rose, F. Savoy *et al.*, 2002 Membrane transport in Caenorhabditis elegans: an essential role for VPS34 at the nuclear membrane. EMBO J. 21: 1673–1683.

Rondon, A. G., M. Garcia-Rubio, S. Gonzalez-Barrera, and A. Aguilera, 2003a Molecular evidence for a positive role of Spt4 in transcription elongation. EMBO J. 22: 612–620.

Rondon, A. G., S. Jimeno, M. Garcia-Rubio, and A. Aguilera, 2003b Molecular evidence that the eukaryotic THO/TREX complex is required for efficient transcription elongation. J. Biol. Chem. 278: 39037–39043.

Rondon, A. G., M. Gallardo, M. Garcia-Rubio, and A. Aguilera, 2004 Molecular evidence indicating that the yeast PAF complex is required for transcription elongation. EMBO Rep. 5: 47–53.

Shilatifard, A., 1998 Identification and purification of the Holo-ELL complex. Evidence for the presence of ELL-associated proteins that suppress the transcriptional inhibitory activity of ELL. J. Biol. Chem. 273: 11212–11217.

Slessareva, J. E., S. M. Routt, B. Temple, V. A. Bankaitis, and H. G. Dohlman, 2006 Activation of the phosphatidylinositol 3-kinase Vps34 by a G protein alpha subunit at the endosome. Cell 126: 191–203.

Stauffer, D. R., T. L. Howard, T. Nyun, and S. M. Hollenberg, 2001 CHMP1 is a novel nuclear matrix protein affecting chromatin structure and cell-cycle progression. J. Cell Sci. 114: 2383–2393.

Straight, A. F., A. S. Belmont, C. C. Robinett, and A. W. Murray, 1996 GFP tagging of budding yeast chromosomes reveals that protein-protein interactions can mediate sister chromatid cohesion. Curr. Biol. 6: 1599–1608.

Swanson, M. J., H. Qiu, L. Sumibcay, A. Krueger, S.-J. Kim *et al.*, 2003 A multiplicity of coactivators is required by Gcn4p at individual promoters in vivo. Mol. Cell. Biol. 23: 2800–2820.

Tietjen, J. R., D. W. Zhang, J. B. Rodriguez-Molina, B. E. White, M. S. Akhtar *et al.*, 2010 Chemical-genomic dissection of the CTD code. Nat. Struct. Mol. Biol. 17: 1154–1161.

Tous, C., A. G. Rondon, M. Garcia-Rubio, C. Gonzalez-Aguilera, R. Luna *et al.*, 2011 A novel assay identifies transcript elongation roles for the Nup84 complex and RNA processing factors. EMBO J. 30: 1953–1964.

Tu, J., L. G. Vallier, and M. Carlson, 1993 Molecular and genetic analysis of the SNF7 gene in Saccharomyces cerevisiae. Genetics 135: 17–23.

Wek, R. C., J. F. Cannon, T. E. Dever, and A. G. Hinnebusch, 1992 Truncated protein phosphatase GLC7 restores translational activation of *GCN4* expression in yeast mutants defective for the eIF-2α kinase GCN2. Mol. Cell. Biol. 12: 5700–5710.

Winzeler, E. A., D. D. Shoemaker, A. Astromoff, H. Liang, K. Anderson *et al.*, 1999 Functional characterization of the *S. cerevisiae* genome by gene deletion and parallel analysis. Science 285: 901–906.

Yeghiayan, P., J. Tu, L. G. Vallier, and M. Carlson, 1995 Molecular analysis of the SNF8 gene of Saccharomyces cerevisiae. Yeast 11: 219–224.

Zhang, F., N. A. Gaur, J. Hasek, S. J. Kim, H. Qiu *et al.*, 2008 Disrupting vesicular trafficking at the endosome attenuates transcriptional activation by Gcn4. Mol. Cell. Biol. 28: 6796–6818.

Communicating editor: K. M. Arndt

GENETICS

Supporting Information
http://www.genetics.org/lookup/suppl/doi:10.1534/genetics.112.146308/-/DC1

Vps Factors Are Required for Efficient Transcription Elongation in Budding Yeast

Naseem A. Gaur, Jiri Hasek, Donna Garvey Brickner, Hongfang Qiu, Fan Zhang, Chi-Ming Wong, Ivana Malcova, Pavla Vasicova, Jason H. Brickner, and Alan G. Hinnebusch

DOI: 10.1534/genetics.112.146308

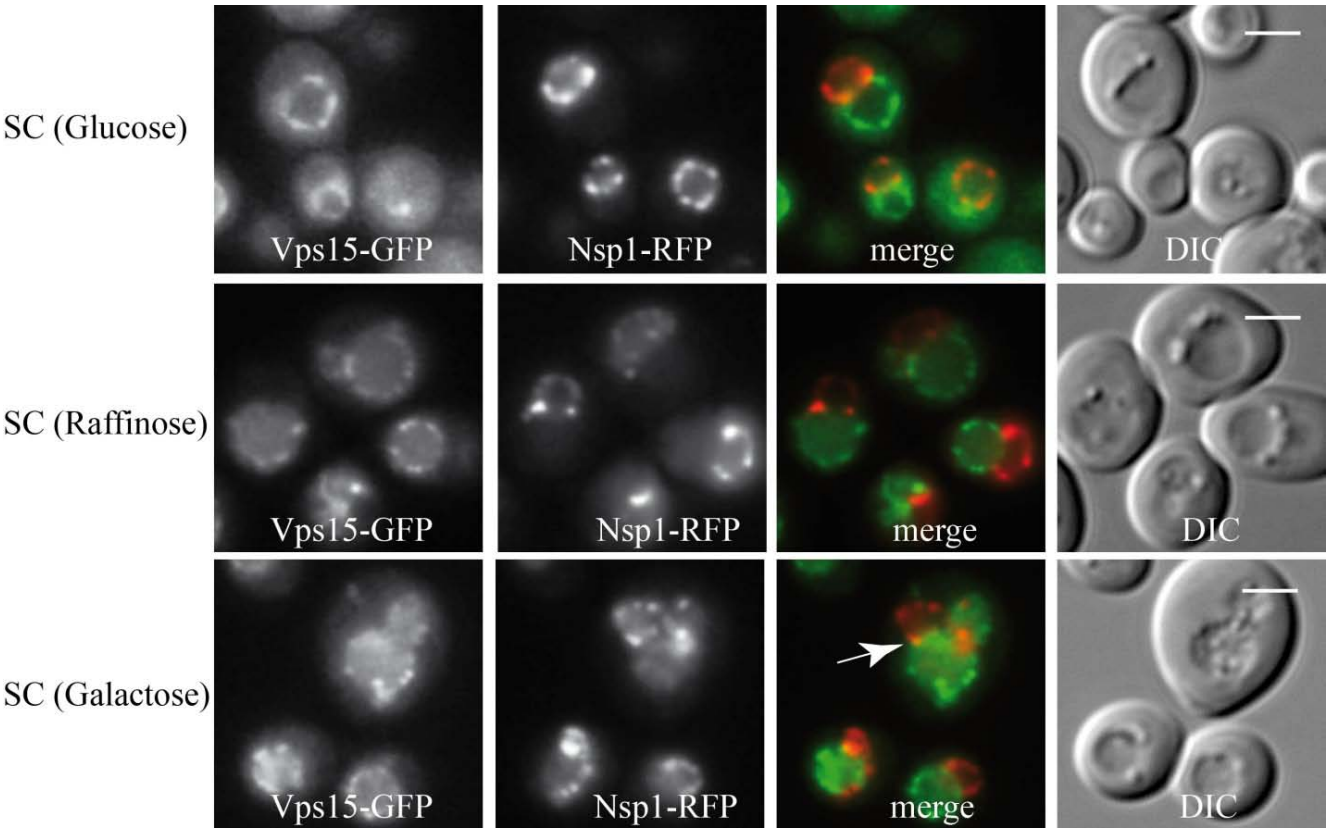

Fig. S1. A fraction of Vps15 associates with nucleoporin Nsp1 at nucleus-vacuole (NV) junctions. Vps15-GFP and nucleoporin Nsp1-RFP were localized in strain CRY1606. Cells were grown overnight at 30°C in SC-Ura medium containing either 2% glucose (SC (Glucose)), or 2% raffinose (SC (Raffinose)), and inspected under coverslips. A portion of cells grown in SC (Raffinose) was transferred to medium containing 2% galactose SC (Galactose), and inspected under coverslips after 5 min incubation. The images show a typical distribution pattern of fluorescence signals observed in a single optical layer in a majority of cells using the Olympus Cell R microscopic system. Scale bar 3μm.

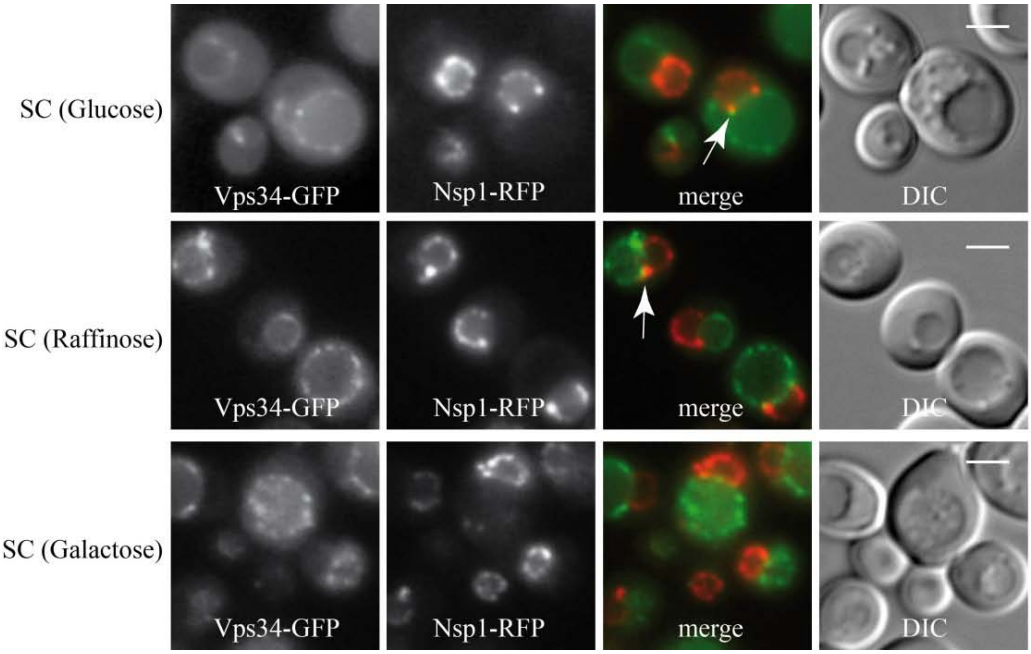

Fig.S2. A fraction of Vps34 also associates with Nsp1 at nucleus-vacuole (NV) junctions. Vps34-GFP and Nsp1-RFP were localized in strain CRY1605. Cells were grown overnight at 30°C in SC (Glucose) or SC (Raffinose) and inspected under coverslips. A portion of cells grown in SC (Raffinose) was transferred to SC (Galactose) and inspected under coverslips after 5 min incubation. The images show a typical distribution pattern of the fluorescence signals observed at a single optical layer in a majority of cells using the Olympus Cell R microscopic system. Scale bar 3μm.

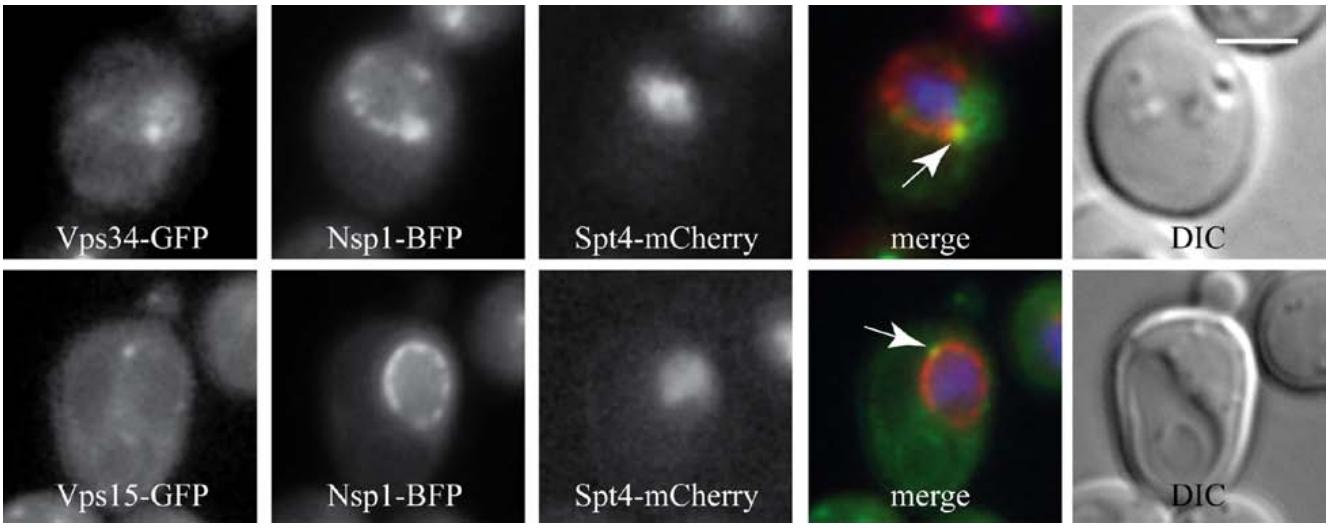

Fig. S3. Vps34 and Vps15 associate with nuclear pores (Nsp1). Cells of strains CRY1718 and CRY1719 grown overnight on YPD plates were inspected under strips of 1.5% agarose in minimal medium containing 2% Galactose using Z-axis optical sectioning by the Olympus Cell R microscopic system. Arrows indicate sites where punctae of Vps34-GFP or Vps15-GFP overlap with Nsp1-BFP punctae in the same optical layer. Such overlaps were found in ca. 50% of ca. 600 cells of each strain scored in several optical layers. False colors (red for BFP and blue for mCherry) were employed to display colocalization sites. Transcription elongation factor Spt4 (Spt4-mCherry) was examined as a specific marker of the nucleoplasm. Scale bar 3μm.

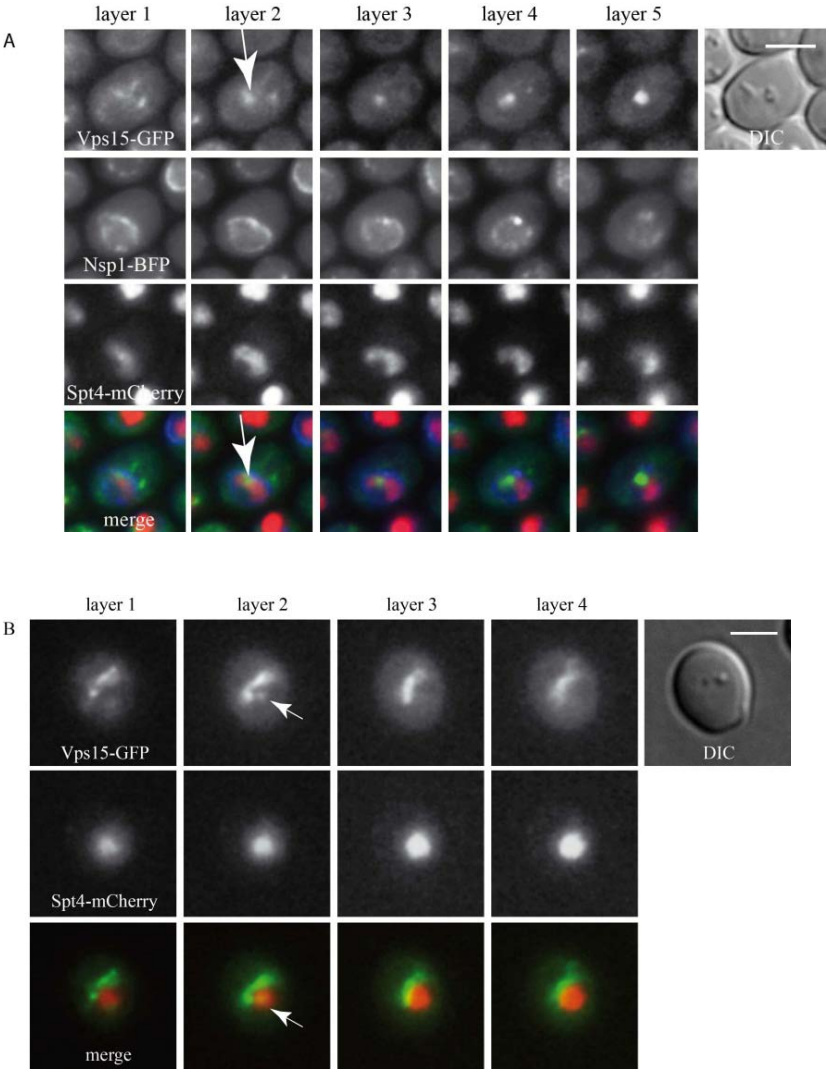

Fig.S4. Rare instances of apparent localization of Vps15 inside the nucleus. (A) Layers 1-5 correspond to different Z-axis sections of the same field of cells of strain CRY1719. The arrow indicates a Vps15-GFP puncta surrounded by Spt4-mCherry within the rim of the nucleus demarcated by Nsp1-BFP. **(B)** Vps15-GFP appears to be accumulated inside the nucleus demarcated by Spt4-mCherry in strain HQY1587. Scale bar 3μm.

Files S1-S6

Videos of time-lapse photography illustrating dynamic association of Vps34-GFP and Vps15-GFP with Nsp1-RFP at the edges of NV junctions

Punctae of Vps34-GFP or Vps15-GFP transiently associate with the nuclear pores delineated by Nsp1-RFP. Cells of strains CRY1605 or CRY1606 were cultured overnight at 30°C in SC (Glucose) (**S1, S2**) or SC (Raffinose) (**S3, S4**) medium. A portion of cells was transferred from SC (Raffinose) to SC (Galactose) medium (**S5, S6**) and cultivated for an additional 60 min. Cells were inspected under coverslips. Fifteen images of the same field were captured by the Olympus Cell R microscopic system in the same optical layer at 10 s intervals between frames. Images were processed by xCellence RT and Adobe CS5 software. ImageJ software was used to export the images as avi movies (5 frames per second).